CISPR TR 16-4-4

Edition 2.0 2020-04

TECHNICAL REPORT

INTERNATIONAL SPECIAL COMMITTEE ON RADIO INTERFERENCE

AMENDMENT 2

Specification for radio disturbance and immunity measuring apparatus and methods –
Part 4-4: Uncertainties, statistics and limit modelling – Statistics of complaints and a model for the calculation of limits for the protection of radio services

CISPR TR 16-4-4:2007-07/AMD2:2020-04(en)

IEC Central Office
3, rue de Varembé
CH-1211 Geneva 20
Switzerland

Tel.: +41 22 919 02 11
info@iec.ch
www.iec.ch

About the IEC
The International Electrotechnical Commission (IEC) is the leading global organization that prepares and publishes International Standards for all electrical, electronic and related technologies.

About IEC publications
The technical content of IEC publications is kept under constant review by the IEC. Please make sure that you have the latest edition, a corrigendum or an amendment might have been published.

IEC publications search - webstore.iec.ch/advsearchform
The advanced search enables to find IEC publications by a variety of criteria (reference number, text, technical committee,…). It also gives information on projects, replaced and withdrawn publications.

IEC Just Published - webstore.iec.ch/justpublished
Stay up to date on all new IEC publications. Just Published details all new publications released. Available online and once a month by email.

IEC Customer Service Centre - webstore.iec.ch/csc
If you wish to give us your feedback on this publication or need further assistance, please contact the Customer Service Centre: sales@iec.ch.

Electropedia - www.electropedia.org
The world's leading online dictionary on electrotechnology, containing more than 22 000 terminological entries in English and French, with equivalent terms in 16 additional languages. Also known as the International Electrotechnical Vocabulary (IEV) online.

IEC Glossary - std.iec.ch/glossary
67 000 electrotechnical terminology entries in English and French extracted from the Terms and definitions clause of IEC publications issued between 2002 and 2015. Some entries have been collected from earlier publications of IEC TC 37, 77, 86 and CISPR.

CISPR TR 16-4-4

Edition 2.0 2020-04

TECHNICAL REPORT

INTERNATIONAL SPECIAL COMMITTEE ON RADIO INTERFERENCE

AMENDMENT 2

Specification for radio disturbance and immunity measuring apparatus and methods – Part 4-4: Uncertainties, statistics and limit modelling – Statistics of complaints and a model for the calculation of limits for the protection of radio services

INTERNATIONAL ELECTROTECHNICAL COMMISSION

ICS 33.100.10; 33.100.20

ISBN 978-2-8322-8224-3

FOREWORD

This amendment has been prepared by CISPR subcommittee H: Limits for the protection of radio services.

The text of this amendment is based on the following documents:

Draft TR	Report on voting
CIS/H/402/DTR	CIS/H/407A/RVDTR

Full information on the voting for the approval of this amendment can be found in the report on voting indicated in the above table.

The committee has decided that the contents of this amendment and the base publication will remain unchanged until the stability date indicated on the IEC website under "http://webstore.iec.ch" in the data related to the specific publication. At this date, the publication will be

- reconfirmed,
- withdrawn,
- replaced by a revised edition, or
- amended.

IMPORTANT – The 'colour inside' logo on the cover page of this publication indicates that it contains colours which are considered to be useful for the correct understanding of its contents. Users should therefore print this document using a colour printer.

2 Normative references

Replace the references to IEC 60050(161) and CISPR 11 with the following:

IEC 60050-161, *International Electrotechnical Vocabulary (IEV) – Part 161: Electromagnetic compatibility* (available at http://www.electropedia.org)

CISPR 11, *Industrial, scientific and medical equipment – Radio-frequency disturbance characteristics – Limits and methods of measurement*

Add the following new reference:

CISPR 15:2018, *Limits and methods of measurement of radio disturbance characteristics of electrical lighting and similar equipment*

3 Terms and definitions

Replace Clause 3 with the following new Clause 3:

3 Terms, definitions, symbols and abbreviated terms

3.1 Terms and definitions

For the purposes of this document, the terms and definitions given in IEC 60050-161 and the following apply.

ISO and IEC maintain terminological databases for use in standardization at the following addresses:

- IEC Electropedia: available at http://www.electropedia.org/
- ISO Online browsing platform: available at http://www.iso.org/obp

3.1.1
complaint
request for assistance made to the RFI investigation service by the user of a radio receiving equipment who complains that reception is degraded by radio frequency interference (RFI)

3.1.2
RFI investigation service
institution having the task of investigating reported cases of radio frequency interference and which operates at the national basis

EXAMPLE Radio service provider, CATV network provider, administration, regulatory authority.

3.1.3
source
any type of electric or electronic equipment, system, or (part of) installation emanating disturbances in the radio frequency (RF) range which can cause radio frequency interference to a certain kind of radio receiving equipment

3.2 Symbols and abbreviated terms

E_{ir}	permissible interference field strength at the point A in space where the antenna of the victim receiver is located – without consideration of probability factors
E_{Limit}	permissible interference field strength at the point A in space where the antenna of the victim receiver is located – with consideration of probability factors
R_P	protection ratio
C_{PV}	coupling factor describing the proportionality of the field strength *E* with the square root of the power *P* injected as common mode into the radiating structure by the apparatus (GCPC)
Group A	defined PV generator group for single-family detached houses
Group B	defined PV generator group for multi-storey buildings with flat roof tops
Group C	defined PV generator group for sun tracking supports (“trees”)
Group D	defined PV generator group for large barns in the countryside
ρ_i	probability of an individual PV generator being a member of Group *i*
$\bar{C}_{PV}$	group-independent mean value for the coupling factor

P_S disturbance power emitted by a GCPC with the complex source impedance Z_S

P_L power injected into the PV generator eventually radiated via that installation

P_{TC} disturbance power determined at the DC-AN on a standardized test site according to CISPR 11 with fixed impedance Z_{TC} = 150 Ω

U_{Limit} permitted disturbance voltage limit

P_7 probability for time coincidence (μ_{P7} in dB)

P_8 probability for location coincidence (μ_{P8} in dB)

P_4 probability for frequency coincidence inclusive harmonics(μ_{P4} in dB)

m_L mismatch loss in use case (between the GCPC with complex source impedance Z_S and the PV generator with complex load impedance Z_L)

m_{TC} mismatch loss in test case (between the GCPC with complex source impedance Z_S and the DC-AN according to CISPR 11 with measurement impedance fixed to Z_{TC} = 150 Ω)

AMN artificial mains network

CM common mode

DC-AN DC artificial network

DM differential mode

GCPC grid connected power converter

S/N noise power/signal power

5.6.5.2.10.2 Estimation for the possible range of μ_{P10}

Add, at the end of 5.6.5.2.10.2, added by Amendment 1, the following new Subclauses 5.6.5.3 and 5.6.5.4:

5.6.5.3 Rationale for determination of CISPR limits for photovoltaic (PV) power generating systems

For a model for the derivation of limits for photovoltaic (PV) power generating systems see Annex C.

5.6.5.4 Rationale for determination of CISPR limits for in-house extra low voltage (ELV) lighting installations

For a model for the estimation of radiation from in-house extra low voltage (ELV) lighting installations see Annex D.

Add, after the existing Annex B, the following new Annex C and Annex D:

Annex C
(informative)

Model for estimation of radiation from photovoltaic (PV) power generating systems

C.1 Overview

This annex presents a model for the estimation of radiation from photovoltaic (PV) power generating systems in the radio frequency range. The model is based on theoretical assumptions, measurement and simulation results as well as on a database with the statistical values of relevant parameters together with appropriate model factors. The simulation results were validated by measurement.

The model was developed for verification of the limits for the LV DC power port of power converters (GCPCs) intended for assembly into PV power generating systems specified in CISPR 11.

The subject of interest was the frequency range below 30 MHz and PV generators with a nominal power throughput in the range up to 20 kVA. Of the two known modes of conducted disturbances, radiation caused by conducted common mode (CM) disturbances was found to be dominant. Therefore the model exclusively considers radiation caused by common mode RF currents (i.e. antenna mode currents).

The structure of this annex is divided into two main parts.

Clause C.2 describes the general model approach mainly consisting of physical rationale, formulae and procedural methods needed for the characterization of the interrelation of the relevant influence factors.

The approach is based on the application of practical data for the various model input parameters gained from measurement, simulation and statistics. Clause C.3 provides the calculation of a resulting limit which serves the primary task of verification of the limits for the LV DC power port of power converters specified in CISPR 11.

C.2 Description of the basic model

C.2.1 Overview

To provide a model suitable for an estimation of radiation from photovoltaic (PV) power generating systems, various influence factors have to be considered.

Figure C.1 gives a schematic overview of the determined influence parameters considered in the model and their interrelation.

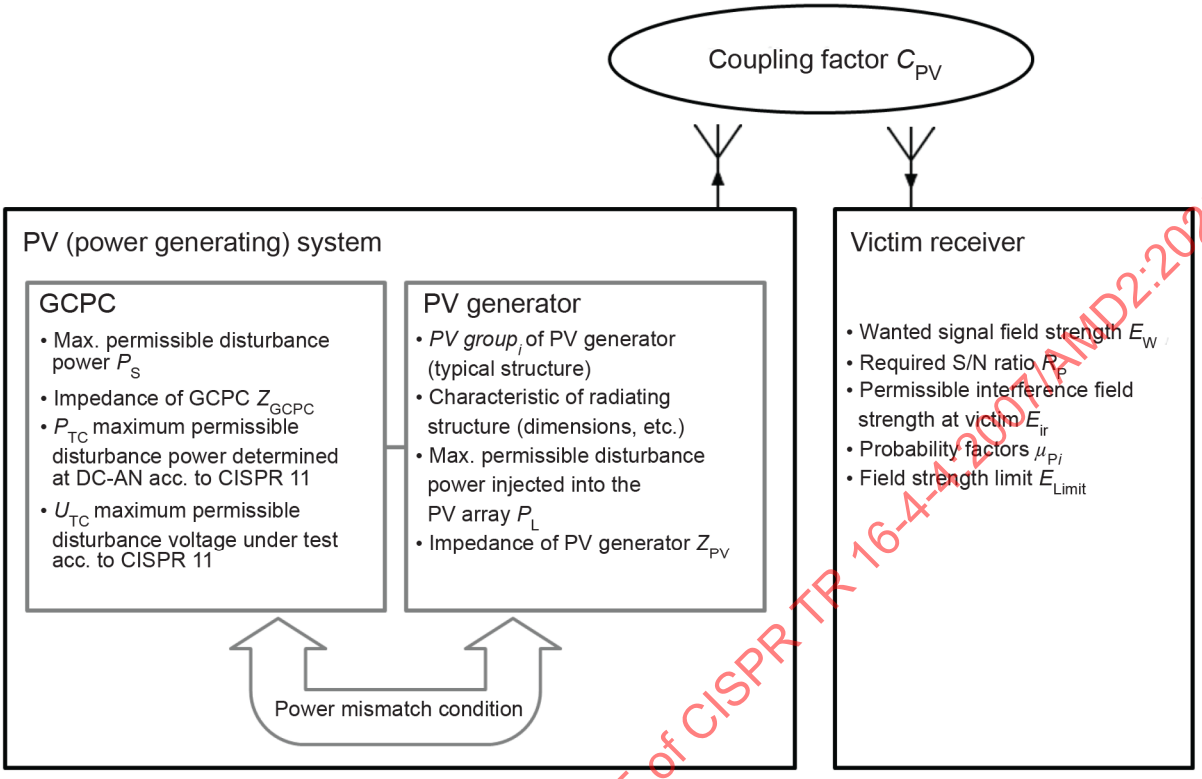

NOTE: For the considerations of the model victim receiver R and measuring receiver M (Figure 2) are identical.

IEC

Figure C.1 – Schematic overview of the considered model influence factors

Initially, the permissible value for the disturbance field strength limit E_{Limit} was determined, at a given point A in space where the antenna of the victim receiver is located, with help of the given formula for the mathematical interrelation of relevant parameters in a remote coupling situation (see C.2.2).

In a second step a model for the PV power generating system was introduced to determine the RFI potential. Subsequently, typical classes of PV power generating systems were selected. Sets of appropriate input parameters for modelling the radiation characteristics were determined (see C.2.3). Those input parameters comprise all the mechanical and electrical data of the solar generator used during its simulation, including electrical permittivity and conductivity of the surrounding ground.

Based on these conventions and assumptions, the coupling between the electromagnetic field at the victim receiver location and the PV generator was characterized by a parameter (introduced as coupling factor C_{PV}). By means of the field strength limit E_{Limit} and this coupling factor C_{PV} the maximum permissible disturbance power P_L injected into the PV generator was estimated. Thereby the basic model for the PV power generating system was completed (see C.2.4).

In addition, the effects of power mismatch losses in test site conditions and at the place of operation of PV power generating systems were used to refine the model (see C.2.5).

C.2.2 Conditions at the location of the antenna of the victim receiver

Considering the technical parameters for reliable transmission and reception of the radio service or application to be protected, the permissible interference field strength E_{ir} (without consideration of probability factors) at the point A in space where the antenna of the victim receiver is located can be determined by subtracting the necessary protection ratio R_P from the minimum wanted field strength E_w needed for this radio reception (see Equation (C.1), all quantities expressed in logarithmic units).

$$E_{ir} = E_w - R_P \tag{C.1}$$

The permissible interference field strength is based on the measurement bandwidth of 9 kHz for the frequency range in question used together with the limit. If the radio service evaluated uses the same bandwidths, as in the case of broadcast radio, no change is necessary. If however the bandwidth of the victim radio service is lower than the measurement bandwidth, a correction shall be applied according to 5.6.6.2 (see Equation (C.2)).

$$E_{ir,corr} = E_{ir} + 10 \times \log\left(\frac{b_{victim}}{b_{measurement}}\right) \tag{C.2}$$

When the calculation of limits for the DC power port of a power converter (GCPC) intended for assembly into a PV power generating system is considered, then only the radiation coupling path to the victim radio receiver needs to be considered. The conductive coupling via the LV AC mains lines is considered to be highly unlikely due to heavy filtering of the AC mains power port of the GCPC.

Equation (37) of this document is the basic calculation rule to gain the permissible disturbance field strength limit E_{Limit} for use with type tests on standardized test sites. The comprehensive formula also includes the various probability factors μ_{Pi} and their corresponding standard deviations σ_{Pi}, reflecting the likelihood of occurrence of a real disturbance in the field, as well as the term $t_\beta \sigma_i$ describing the predefined statistical significance of CISPR limits for type-approved appliances. Combining Equation (37), Equation (C.1) and Equation (C.2) leads to Equation (C.3):

$$E_{Limit} = E_{ir,corr} + \mu_{P1} + \ldots + \mu_{P10} + t_\beta \sigma_i - t_\alpha \sqrt{\sigma_{P1}^2 + \ldots + \sigma_{P10}^2} \tag{C.3}$$

NOTE 1 Suitable probability factors for PV power generating systems are defined depending on the context of application (see C.3.3).

NOTE 2 This document is based on the assumption that the signal characteristics of disturbances caused by PV systems in its worst case are continuous, leading to equivalent outputs of all CISPR detectors.

Once the field strength limit E_{Limit} is found, a coupling factor C_{PV} comprising the coupling characteristics between the electromagnetic field at the victim receiver location and the PV power generating system can be applied to estimate the maximum permissible disturbance power P_L that can be injected into a given PV generator (see C.2.4).

C.2.3 Characteristics of PV generators

C.2.3.1 General

In this Subclause C.2.3 a model for the PV power generating system is introduced to determine the permissible RFI potential. Subsequently, typical classes of PV power generating systems are selected. Sets of appropriate input parameters for modelling of their radiation characteristics are determined.

C.2.3.2 Characteristic parameters of a PV generator seen as radiator of RF disturbances

In a simplified approach, a typical PV power generator can be regarded as an ideal vertical rod antenna with capacitive top loading. The DC power string wires are treated as antenna, while the PV panels or modules make up its capacitive loading. This approach is applicable for common mode radiation only, but several investigations indicated this radiation to be predominant in the considered case.

For the specified power range (i.e. up to 20 kVA) typical PV generator configurations can be found in large numbers. On a single-family detached house some PV panels are mounted on the inclined roof. For multiple-family houses very often a flat top roof can be found carrying rows of PV panels on its top. A sun tracker, which is made up by a singular steel support carrying some PV panels that always present their broad side to the sun, and fairly large generators on barns in the countryside, are also fairly common.

As consideration of every individual PV generator configuration is not feasible, group representatives of PV generator types are introduced (see C.2.3.3).

Subclause C.3.4 reveals the technical parameters that were assumed and used in the simulation for calculation of the RF characteristics of the respective group of PV generators.

C.2.3.3 Grouping of PV generators

For every individual photovoltaic power generating system or installation, the individual coupling property C_{PV_i} may assume a different value, but it can be expected that PV generators with about the same geometric structure and size, will show a typical property C_{PV_i} allocated somewhere in a given (predictable standard deviation) range.

As PV generators occur in various different configurations in the field, it was decided to define group representatives of PV generator types and to create a model for each group leading to different coupling factors $C_{\text{PV Group } i}$ (see C.3.4), describing the interrelation between the victim receiver and the respective assumed group or category of PV generators.

The defined PV generator groups are:

Group A – Single-family detached houses;

Group B – Multi-storey buildings with flat roof tops;

Group C – Sun tracking supports (“trees”);

Group D – Large barns in the countryside.

Assuming the properties of all photovoltaic power generators in the world are known and that every individual one of those can be put into one of the predefined groups which is represented by its model or type (and thus has C_{PV_i} as a describing constant) it can be defined that

$$\rho_i = \frac{\text{Nb of PV generators in group } i}{\text{Nb of PV generators in the world}} \tag{C.4}$$

where ρ_i represents the probability of an individual PV generator being a member of group *i*, while the respective coupling factor C_{PV_i} describes the typical RF characteristics of this group (see Figure C.2).

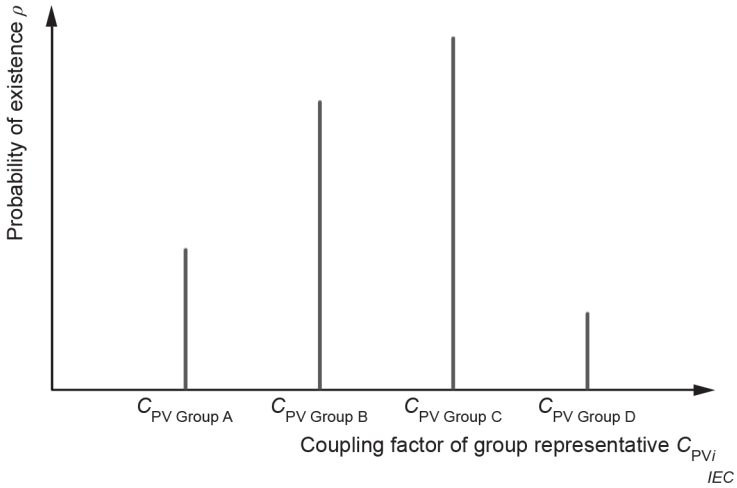

Figure C.2 – Schematic representation of probability of existence of PV generator groups in the field

Statistical data on the population density of the PV generators in the field is given in C.3.4.3.2.

From this data, a group-independent mean value for the coupling factor $\overline{C}_{PV}$ and its variance $\overline{\sigma}_{PV}$, which is valid and typical for any PV generator configuration, can be deduced (see Figure C.3).

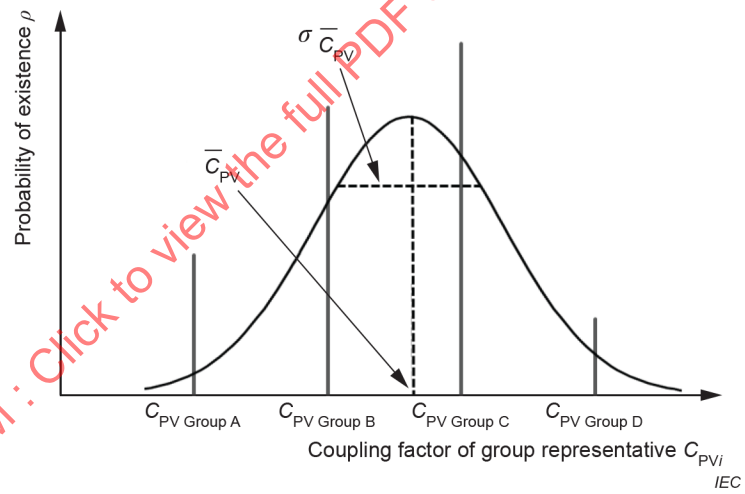

Figure C.3 – Schematic representation of mean value $\overline{C}_{PV}$ and variance σ_{CPV}

The global (or mean) value $\overline{C}_{PV}$ can be calculated by Equation (C.5):

$$\overline{C}_{PV} = \sum_{\text{all groups}} C_{PV} \times \rho_i \qquad \text{(C.5)}$$

This simplified value $\overline{C}_{PV}$ for the global coupling factor is needed to select the type-independent limit $U_{TC\ Limit}$ for the LV DC power port of power converters (GCPCs) specified in CISPR 11 (see Clause C.3 of this document).

C.2.3.4 Electrical input parameters of the PV generator

One intermediate step of the approach is the determination of the maximum permissible disturbance power P_L that may be injected into the PV generator. In power matching conditions, this P_L is identical with the permissible disturbance power P_S provided by the GCPC.

For thorough estimation of the RFI potential, the typical power mismatch loss between the GCPC and the DC power interface of the respective PV generator has to be taken into account which requires knowledge of the complex impedances of GCPCs and PV generators (see C.2.5).

C.2.4 Coupling between the electromagnetic field at the victim receiver location and PV power generating system

C.2.4.1 General

When assessing the disturbance potential of any given apparatus with any attached structure, the relationship between the disturbance field strength E_{Limit} at a given point A in space and the RF power P_L fed into the radiating structure by the given apparatus has to be determined. The relevant technical parameter or characteristic of a given PV generator is its frequency dependent coupling factor C_{PV}.

For this task, the disturbance source, i.e. the grid connected power converter (GCPC) can be modelled as a common mode power generator that injects a certain power P into a radiating structure through its DC power port. The AC power port connects directly or via the PE conductor in the AC mains cable local ground as the counterpoise of the radiating structure. A block scheme covering this situation is shown in Figure C.4.

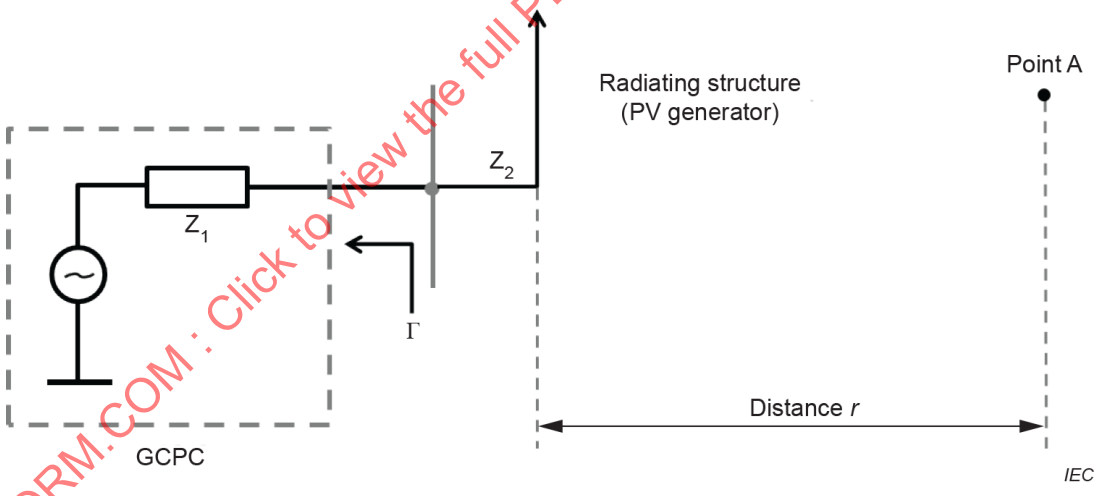

Figure C.4 – General model for coupling of CM disturbances of a GCPC to an attached photovoltaic power generating system (PV generator)

In a first approach the observation point A in space is assumed to be located at a fixed distance r from the PV generator. The electrical (disturbance) field strength E of the electromagnetic field emanating from the radiating structure is proportional to the square root of the real power P fed into the PV generator, due to the linearity of Maxwell's equations.

For a single point in space, a fixed function $C_{PV} = C_{PV}(f)$ (coupling factor) describes the proportionality of the field strength E with the square root of the power P injected into the radiating structure by the apparatus (GCPC), as given in Equation (C.6).

$$E = C_{PV} \times \sqrt{P} \tag{C.6}$$

For EMC considerations the situation at a fixed distance (e.g. the CISPR protection distance of 10 m or 30 m) is needed. For real objects many points in space with the property of having a given distance to the EUT exist, for example in different azimuth directions and at different heights. This applies to simulation and measurement equally. Therefore the field strength used in Equation (C.6) shall undergo some kind of maximization procedure before being used for the calculation of the coupling factor. Henceforward this parameter C_{PV} covers the worst case radiation properties/characteristics of the model for the fixed installation and is explicitly valid for one given fixed distance r and one specific group (A, B, C or D) of PV generators. By means of Equation (C.7) the maximum permissible disturbance power that may be injected into the PV generator P_L can be calculated to:

$$P_L = \frac{E_{Limit}^{\ 2}}{C_{PV}^{\ 2}} \tag{C.7}$$

Basically, it does not matter whether a victim receiver's antenna picks up either the electric or the magnetic portion of the radiated disturbance and which of the two coupling mechanisms is predominant for the respective distance. They differ, because for most frequencies the victim receiver is in the near field zone of the radiating structure.

Using the coupling factor for the electric field strength and the magnetic field strength to calculate the resulting field strengths appearing at the point in question, it can be seen, that the two coupling factors can be compared to each other in the same unit (Equation (C.8)). The disturbance field strengths, which are compared to each other and to the field strength of the radio service, are in the far field of the transmitter.

$$\left.\begin{aligned} E &= C_{PV\,elec} \cdot \sqrt{P} \\ H &= C_{PV\,mag} \cdot \sqrt{P} \end{aligned}\right\} \rightarrow \frac{E}{H} = \frac{C_{PV\,elec}}{C_{PV\,mag}} \tag{C.8}$$

By multiplying the coupling factor for the magnetic field $C_{PV\,mag}$ with the free space impedance Z_0, the results can be compared in the same units. Note that the coupling factor for the magnetic fields will also be given in the unit $\sqrt{\Omega}/\mathrm{m}$ (see Equation (C.9)).

$$C_{PV\,elec}\left[\frac{\sqrt{\Omega}}{\mathrm{m}}\right] = C_{PVmag}\left[\frac{1}{\mathrm{m}\cdot\sqrt{\Omega}}\right] \cdot Z \tag{C.9}$$

NOTE Generally electric and magnetic fields are not interrelated by the free space impedance Z_0 in the near field.

By convention, the coupling factor for the required protection distance is defined as the mean value of all field strengths determined for a number of points in the xy-plane at the required distance. When only four spatial directions are assessed, the final values of the coupling factor can be calculated by

$$\begin{aligned} C_{PV\,elec} &= \mathrm{mean}(\, C_{PV\,elec\,0°}, C_{PV\,elec\,90°}, C_{PV\,elec\,180°}, C_{PV\,elec\,270°}\,) \\ C_{PV\,mag} &= \mathrm{mean}(\, C_{PV\,mag\,0°}, C_{PV\,mag\,90°}, C_{PV\,mag\,180°}, C_{PV\,mag\,270°}\,) \end{aligned} \tag{C.10}$$

In a last step the predominant coupling (electric or magnetic) is found by maximization.

$$C_{PV} = \max(C_{PV\,elec}, C_{PV\,mag} \times Z_0) \quad \text{(C.11)}$$

C.2.4.2 Determination of coupling factor by simulation $C_{PV\,sim}$

One approach to determine the coupling factor is to carry out simulations with a Maxwell equation solver (i.e. NEC2, FEKO, Concept).

Taking a defined representative geometrical configuration for each PV generator group as basis, a relationship between the injected disturbance power and the resulting radiated disturbance field strength in a point A in space at a defined distance from the PV generator can be found.

The main input for the simulation is the geometry of the photovoltaic generator. This mechanical structure needs to be programmed into the simulating engine. An example is shown in Figure C.5.

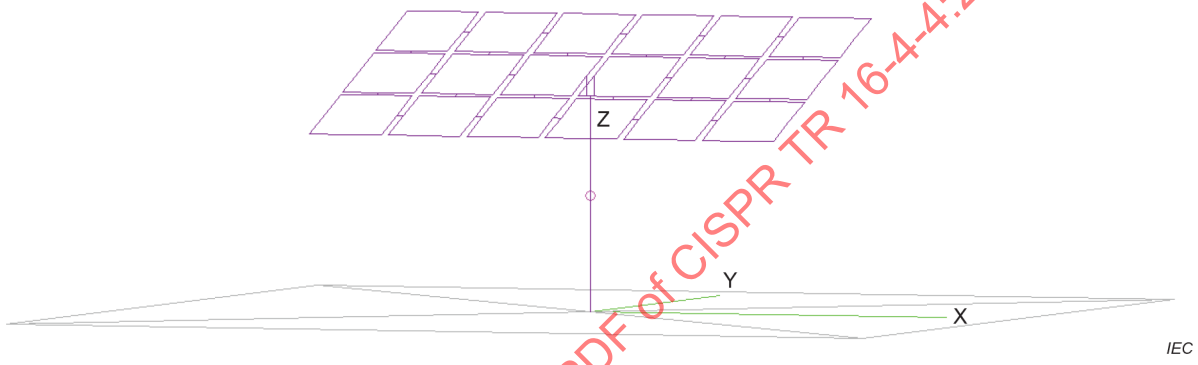

Figure C.5 – Geometric representation of a PV generator with 18 modules

In the defined structure, common mode power is injected at the feed point (indicated by a purple circle in the middle of the feed line) and the field strength is calculated in a cuboid around the structure. The distance from the structure at which the coupling factor C_{PV} shall be calculated determines the size of the cuboid in x and y directions. The protection distance in CISPR standards is often 3 m, 10 m or 30 m. For a large structure like a photovoltaic array, calculations for the protection distance of 3 m are not used for the example presented in this document. The size of the cuboid in vertical z direction shall be twice the height of the structure itself.

The output of the simulation is the field strength on the surface of the pre-programmed cuboid. Choosing a point on the xy-plane at a distance corresponding to the required protection distance defines a vertical line (see Figure C.6).

Dimensions in metres

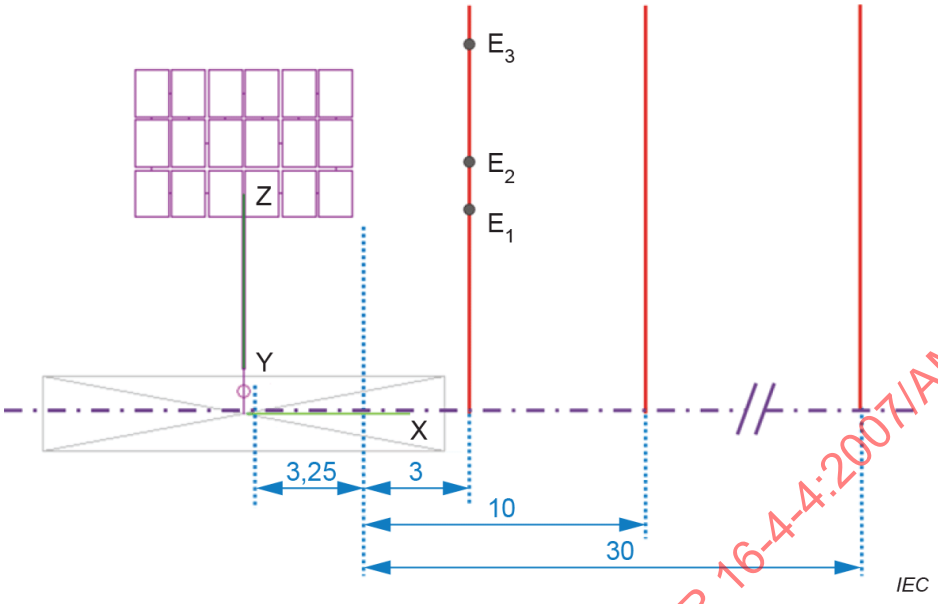

Figure C.6 – Field strength determination by maximization (height scan) along a red line

The maximum of all field strengths in the cross-section between this line and the cuboid represents the final field strength for the distance. Ideally this procedure would be repeated for each angular direction, however it suffices to consider only the four different orthogonal directions in space. The coupling factor $C_{PV\ sim}$ is then derived according to Equations (C.10) and (C.11).

C.2.4.3 Determination of coupling factor by measurement $C_{PV\ meas}$

The coupling factor introduced by Equation (C.6) can also be determined by measurement. However, as the coupling factor is defined in transmission mode, it is difficult to measure the field strength distribution around a typical setup for a PV generator, since the setup is too large for accurate measurement in most available shielded rooms. On the other hand it is not possible to actually transmit a potential test signal on any frequency at the installation site of a PV generator, because of national restrictions. However, under specific operating conditions (e.g. limitation of transmission to suitable single test frequencies) a measurement on real installations is feasible.

For these measurements, the DC wires of the PV generator shall be disconnected from the GCPC, shorted and connected to a typical antenna tuner. The tuner should be grounded the same way an installed GCPC would be grounded. The tuner shall be able to tune the feed point impedance of this “antenna” to the 50 Ω output of the transmitter at all test frequencies, such that only very little RF reflection occurs. The actual forward and reflected power shall be measured and monitored during the procedure with a power meter.

The field strength shall then be measured at a pre-defined fixed distance from the outer boundary of the PV installation (e.g. at 10 m or 30 m). The measurement should be made in the four dominant perpendicular directions at heights starting from 1 m above ground level up to twice the installation height. If this cannot be achieved, the measurement can be simplified to fewer directions and lower and fewer heights.

A comprehensive result table of this suite of measurements shall provide the following information:

1) frequencies used for testing;

2) location (distance r from the boundary of the PV generator, orientation in 90° angles and height above ground);
3) forward and reflected power to determine the radiated power P_L (power mismatch considered);
4) total electric and magnetic field-strength (derived from the x, y, and z components);
5) ambient noise level of electric and magnetic field strength;
6) determined maximum value of the field strength reading obtained in each height;
7) determined mean of the measured field strength values E_{meas} and H_{meas}, between for example the four perpendicular directions used for the measurements;
8) evaluation result: maximum of measured coupling factors $C_{PV\ elec\ meas}$ and $C_{PV\ mag\ meas}$.

The respective coupling factors can be calculated from the test results by means of Equations (C.10) and (C.11).

C.2.4.4 Validation of simulation results with measurements

Comparison of measurement and simulation results will always show discrepancies. On the one hand reasonable simulation does not seek to reproduce reality completely (input parameters will be simplified or in some cases will not be sufficiently known), but focusses on the assumed main influence factors. On the other hand, measurements are also influenced by unwanted factors (uncertainty characteristics of the test equipment, environmental influences in situ, limited height scan capabilities, access problems in different azimuth directions, etc.), especially in the case of the complex test setup referred to in this annex.

To check and increase the accuracy of the simulation, measurements on several PV generator structures shall be performed to verify the simulation results (see C.3.4).

C.2.5 Considerations of power mismatch losses

C.2.5.1 General

Subclause C.2.5 contains mathematical considerations regarding the usual power mismatch conditions between the PV generator and the GCPC at the installation site of the PV generator.

In addition, the power matching conditions between the GCPC and the DC-AN in the test case according to CISPR 11 can be considered. This allows conclusions to be drawn from ordinary GCPC type test data about the maximum disturbance power P_S of the GCPC deliverable in a given installed PV generator.

Due to the representation of test site conditions (Equation (C.15)) in the measurement uncertainty and the lack of the representation of the relationship between the maximum permissible power in the test case and in the installation case (Equation (C.16)) in any other investigations (e.g. radiation from AC mains grid networks), this option can be added if this scenario type is required. But then the related factors, for example measurement uncertainty or AC mains, grid investigations and limits may have to be adjusted in a similar way.

C.2.5.2 Power mismatch conditions at the installation site of the PV power generating system

In practice there is a certain loss of power compared to power matching conditions between source and load, when the source of RF disturbances, in this case the PV power converter (GCPC), is connected to an RF load, in this case the installed PV generator.

This quantity is denoted as the mismatch loss m_L and can be considered as a real attenuation. For a GCPC with the complex source impedance Z_S emitting a disturbance power P_S into the

PV generator with the complex load impedance Z_L, the complex reflection coefficient Γ and the final loss can be calculated by Equation (C.12).

$$\Gamma = \frac{Z_L - \bar{Z}_S}{Z_L + Z_S}$$
$$m_L = 1 - |\Gamma|^2 \qquad \text{(C.12)}$$
$$M_L = 10 \cdot \log\left(1 - |\Gamma|^2\right)$$

The actual power P_L injected into the PV generator, which is mainly radiated via that installation, is therefore reduced to (see Equation (C.13)):

$$P_L = m_L \cdot P_S \qquad \text{(C.13)}$$

If P_L is known, then the maximum permissible disturbance power P_S that can be injected by the GCPC can be calculated with Equation (C.13).

Subclause C.3.6 gives some statistical data of impedances of PV generators (Z_L) and GCPCs (Z_S) to enable the determination of m_L.

C.2.5.3 Power mismatch conditions at the test site

In general, P_S will not be known, but can be derived from a measurement of P_{TC} on a standardized test site according to CISPR 11. The measurement impedance is fixed to Z_{TC} = 150 Ω, due to the technical parameters of the DC-AN, while the power converter still has the complex source impedance Z_S. Measuring P_{TC} in the test case (i.e. the disturbance power determined at the DC-AN) the unknown P_S can be calculated by

$$P_{TC} = m_{TC} \cdot P_S \qquad \text{(C.14)}$$

with m_{TC} being described by

$$\Gamma_{TC} = \frac{150\,\Omega - \bar{Z}_S}{150\,\Omega + Z_S}$$
$$m_{TC} = 1 - |\Gamma_{TC}|^2 \qquad \text{(C.15)}$$

C.2.5.4 Conclusion to test conditions

The relationship between the maximum permissible power in the test case P_{TC} and in the installation case P_L is given by the ratio of the two mismatch losses (Equation (C.16)):

$$\frac{P_{TC}}{P_L} = \frac{m_{TC}}{m_L} \qquad \text{(C.16)}$$

The maximum permissible disturbance power P_S of the power converter (GCPC) is always higher than or equal to the measurement result in the test case, as both mismatch factors work

one against the other. If the PV generator actually has an input impedance of 150 Ω, then m_{TC} and m_L are equal and cancel out.

If P_{TC} is known, the respective limit for the permitted disturbance voltage at the DC power port of the GCPC can be calculated using the following relation (Equation (C.17)):

$$U_{\text{Limit}}\left[\text{V}\right] = \sqrt{150\Omega \times P_{TC}\left[\text{W}\right]}$$
$$U_{\text{TC Limit}}\left[\text{dB}\left(\mu\text{V}\right)\right] = 20 \times \log_{10}\left(\frac{U_{\text{Limit}}\left[\text{V}\right]}{1\mu\text{V}}\right) \quad \text{(C.17)}$$

C.3 Calculation based on practical values for the verification of the limits specified in CISPR 11

C.3.1 General

Clause C.3 presents a calculation based on practical values gained by measurement, simulation and statistical data for the introduced parameters of the model, to fulfil the primary task of the verification of the limits for the LV DC power port of power converters intended for assembly into PV power generating systems specified in CISPR 11.

The following list gives an overview of the parameters needed for the verification for a given radio service or application. The following subclauses will describe in detail the assumptions made to gain concrete values for the calculation.

- wanted signal field strength E_w;
- required S/N respectively protection ratio R_P;
- probability for time coincidence P_7;
- probability for location coincidence P_8;
- probability for frequency coincidence inclusive harmonics P_4;
- global coupling factor $\overline{C}_{PV}$;
- test site correction m_{TC};
- mismatch loss at installed PV generator m_L.

Some quantities, for example t_α = 0,84 and t_β = 0,84 used in this Clause C.3 to calculate validation values in accordance with Clause C.2, are defined in the main clauses of this document. Furthermore σ_i, which describes the predefined statistical significance of CISPR limits for type-approved appliances, was set to zero, as the application of the 80/80-rule was discontinued.

C.3.2 Determination of the maximum permissible interference field strength E_{ir} at the location of the antenna of the victim receiver

The maximum permissible interference field strength E_{ir} for the disturbance is determined by subtracting the protection ratio from the wanted signal field strength of the radio application. Usually these parameters are given in ITU-R publications, but for simplicity CISPR has collected and published the results in the "Radio Services Database" on the IEC website under the EMC technology sector.

Here the radio application to be protected is chosen to calculate the permissible disturbance field strength E_{ir} by using Equation (C.1).

EXAMPLE A wanted signal field strength E_w = 44 dB(µV/m) and a necessary signal-to-noise or protection ratio R_P = 27 dB is taken, for good radio reception from a radio broadcast AM transmitter operating in the 31 m RF band.

This has to be evaluated for every entry in the radio services database resulting in a function for E_{ir} dependent on the frequency.

C.3.3 Probability factors

C.3.3.1 General

The disturbance will not actually occur in all cases, due to the fact that victim and source need to coincide in time, location and frequency. These three probability factors are assumed to play the major role in a disturbance scenario with a PV power generating installation.

When logarithmic probability factors are calculated, the linear probability shall be converted to a logarithm in base 10 and multiplied with a factor of 10, which originates from the signal-to-disturbance ratio defined as ratio of received signal power to the received disturbance power. Solely for distance ratios a factor of 20 shall be used.

C.3.3.2 Probability factor for time coincidence μ_{P7} and σ_{P7}

The disturbance can only occur at times, when the PV power generating system is in operation. The average day time is 12 h, but the production of energy is a bit less, due to mounting of the solar modules on an inclined plane. As an average of time 10 h are chosen, as the majority of installations are of this kind (Equation (C.18)).

$$\mu_{P7} = 10 \times \log_{10}\left(\frac{10}{24}\right) = 3{,}8 \text{ dB} \tag{C.18}$$

However, there are some other installation types also present, such as sun trackers or flat mounted modules. Therefore the “in operation” interval can vary in a wide range between 4 h and 20 h per day following an assumed uniform distribution that can be calculated by Equation (C.19):

$$\sigma_{P7} = -\frac{10 \times \log_{10}\left(\frac{20}{24}\right) - 10 \times \log\left(\frac{4}{24}\right)}{2 \times \sqrt{3}} = 2 \text{ dB} \tag{C.19}$$

C.3.3.3 Probability factor for location coincidence μ_{P8} and σ_{P8}

Conclusions on a representative probability factor for location coincidence were drawn based on data from Germany using information from the statistical data used for the determination of the coupling factor.

The value of 1,038 million photovoltaic installations registered combined with the amount of 40,96 million households (data status 2015) leads to a photovoltaic installation density of about 2,5 %. Taking into account future growth, a value of 1,6 million PV systems is taken as basis for the calculation leading to a density of 4 %. It is assumed that every house has four neighbours (front, rear, left and right) within the protection distance. However the total number of installations can vary (e.g. depending on other factors such as national funding), so photovoltaic installation densities in the field between 2 % and 8 % are assumed. Moreover, it is assumed that there is radio broadcast reception in every household.

These assumptions lead to Equation (C.20):

$$\mu_{P8\,PV} = -10 \times \log_{10}(4 \times 0{,}04) = 8\ \text{dB} \tag{C.20}$$

$$\sigma_{P8\,PV} = -\frac{10 \times \log_{10}(4 \times 0{,}02) - 10 \times \log_{10}(4 \times 0{,}08)}{2} = 3\ \text{dB} \tag{C.21}$$

However, there is only one amateur station in every thousand households in a world average. Therefore an additional location coincidence shall be applied in the case of the amateur radio service.

$$\mu_{P8\,AmaR} = -10 \times \log_{10}(0{,}001) = 30\ \text{dB} \tag{C.22}$$

$$\sigma_{P8\,AmaR} = -\frac{10 \times \log_{10}(0{,}0005) - 10 \times \log_{10}(0{,}005)}{2} = 5\ \text{dB} \tag{C.23}$$

C.3.3.4 Probability factor for frequency coincidence μ_{P4} and σ_{P4}

The frequency probability can be estimated by considering typical disturbance spectra of GCPCs.

Assuming that about 3 MHz out of the 30 MHz are occupied by emission, this leads to Equation (C.24):

$$\mu_{P4} = -10 \times \log_{10}\left(\frac{3}{30}\right) = 10\ \text{dB} \tag{C.24}$$

As the characteristic spectra of GCPCs vary across a broad range, a rather high uncertainty needs to be assigned, which leads to an assumption according to Equation (C.25):

$$\sigma_{P4} = 5\ \text{dB} \tag{C.25}$$

C.3.3.5 Maximum permissible field strength E_{Limit} considering probability factors

For every calculated E_{ir} according to C.3.2 the probability factors are applied using Equation (C.3) and result in a frequency dependent E_{Limit}.

EXAMPLE 1 In the case of the shortwave radio broadcast service in the 31-m-band introduced in C.3.2, with the wanted field strength of 44 dB(µV/m) and its protection ratio of 27 dB, taking into account the probability factors and their distributions (C.3.3.2 to C.3.3.4) a maximum permissible field strength of 33,6 dB(µV/m) can be calculated.

$$\begin{aligned} E_{Limit} &= E_W - R_P + \mu_{P4} + \mu_{P7} + \mu_{P8} + t_\alpha \cdot \sqrt{\sigma_{P4}^2 + \sigma_{P7}^2 + \sigma_{P8}^2} \\ &= \left(44 - 27 + 10 + 3{,}8 + 8 - 0{,}84 \cdot \sqrt{5^2 + 2^2 + 3^2}\right)\text{dB}\,(\mu\text{V/m}) = 33{,}6\,\text{dB}\,(\mu\text{V/m}) \end{aligned}$$

EXAMPLE 2 In the case of the amateur radio service in the 20-m-band, with a sensitivity of -11 dB(µV/m) and its protection ratio of 10 dB, taking into account the probability factors and their distributions (C.3.3.2 to C.3.3.4) a maximum permissible field strength of 29,4 dB(µV/m) can be calculated.

$$E_{\text{Limit}} = E_{\text{W}} - R_{\text{P}} - 10 \cdot \log_{10}\left(\frac{b_{\text{victim}}}{b_{\text{measurement}}}\right) + \mu_{\text{P4}} + \mu_{\text{P7}} + \mu_{\text{P8}} + t_{\alpha} \cdot \sqrt{\sigma_{\text{P4}}^2 + \sigma_{\text{P7}}^2 + \sigma_{\text{P8}}^2}$$

$$= \left(-11 - 10 - 10 \cdot \log_{10}\left(\frac{2700}{9000}\right) + 10 + 3{,}8 + 38 - 0{,}84 \cdot \sqrt{5^2 + 2^2 + 6^2}\right) \text{dB}(\mu\text{V/m}) = 29{,}4\,\text{dB}(\mu\text{V/m})$$

C.3.4 Global coupling factor $\overline{C}_{\text{PV}}$

C.3.4.1 Determination of coupling factors $C_{\text{PV}\,i\,\text{sim}}$ by simulation

C.3.4.1.1 General

Subclause C.3.4.1 gives the simulation results for the predefined groups of typical PV generators in the power range up to 20 kVA at a distance of 10 m from the outer boundary exclusively.

The following simulations (except for Group C) have been performed with the NEC2 calculating engine with a Sommerfeld ground model (conductivity σ = 5 mS/m and permittivity ε_r = 13). Due to this, direct connection to ground is not feasible and a certain capacitive coupling has been introduced using radial wires.

C.3.4.1.2 Simulation results for the coupling factor $C_{\text{PV Group A sim}}$ – Group A (Single-family detached houses)

For this simulation the average array height of the photovoltaic generator was assumed to be 6 m and with a tilt angle of 37°. In the model, the connection of the DC wires goes directly to the frame of the modules. Alternatively the whole PV panel structure can be simulated as a complete wire mesh forming a tilted rectangular plane with dimensions of 6 m × 4,5 m. The position of the PV power converter (GCPC) was assumed to be near the ground. See Figure C.7 and Figure C 8.

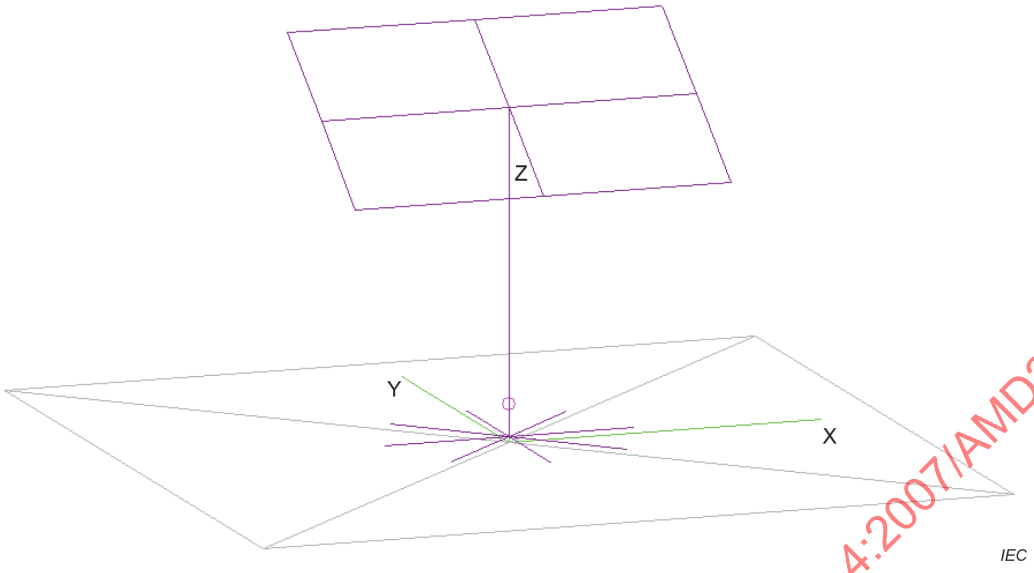

Figure C.7 – Geometrical representation of Group A PV generators

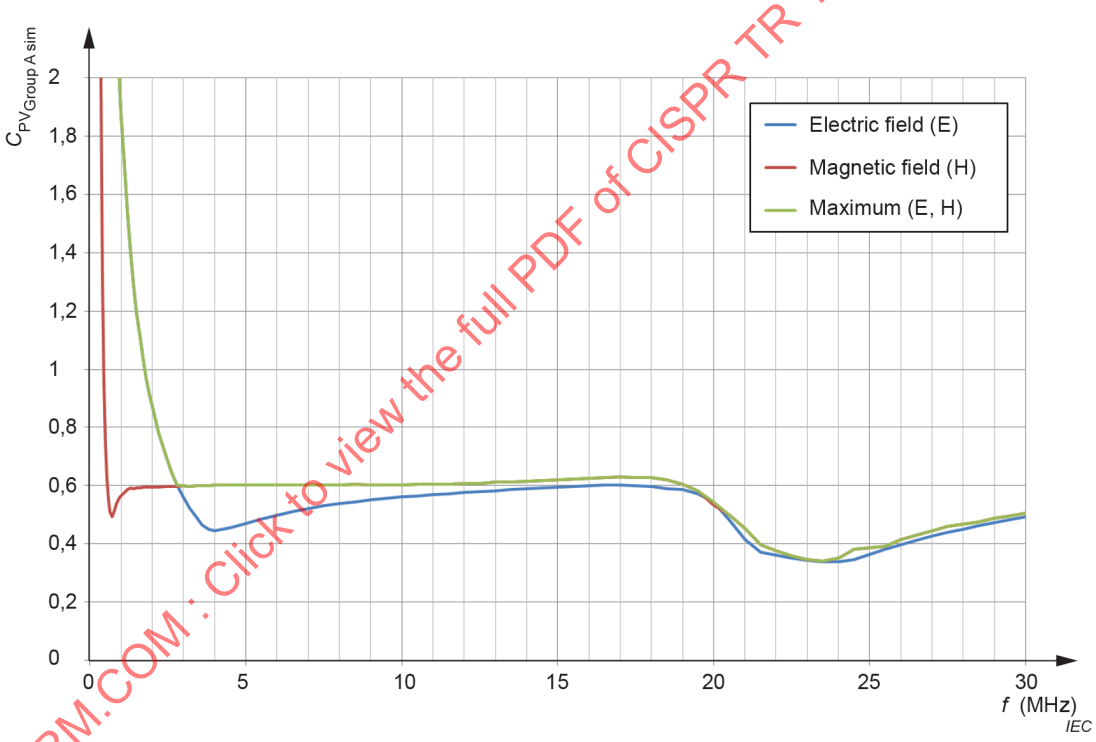

Figure C 8 – Combined coupling factor $C_{PV\,Group\,A\,sim}$ for Group A PV generators (r = 10m)

C.3.4.1.3 Simulation results for the coupling factor $C_{PV\,Group\,B\,sim}$ – Group B (Multi-storey house)

For this simulation the total resulting power of the photovoltaic system was assumed to be around 19 kVA, while the panels are practically installed on a flat top house of height 12 m. The house was simulated with four lightning protection wires down and connected to the ground at each corner. The position of the photovoltaic inverter is on the flat roof and driven against a conduction frame grounded by the lightning protection wires. See Figure C.9 and Figure C.10.

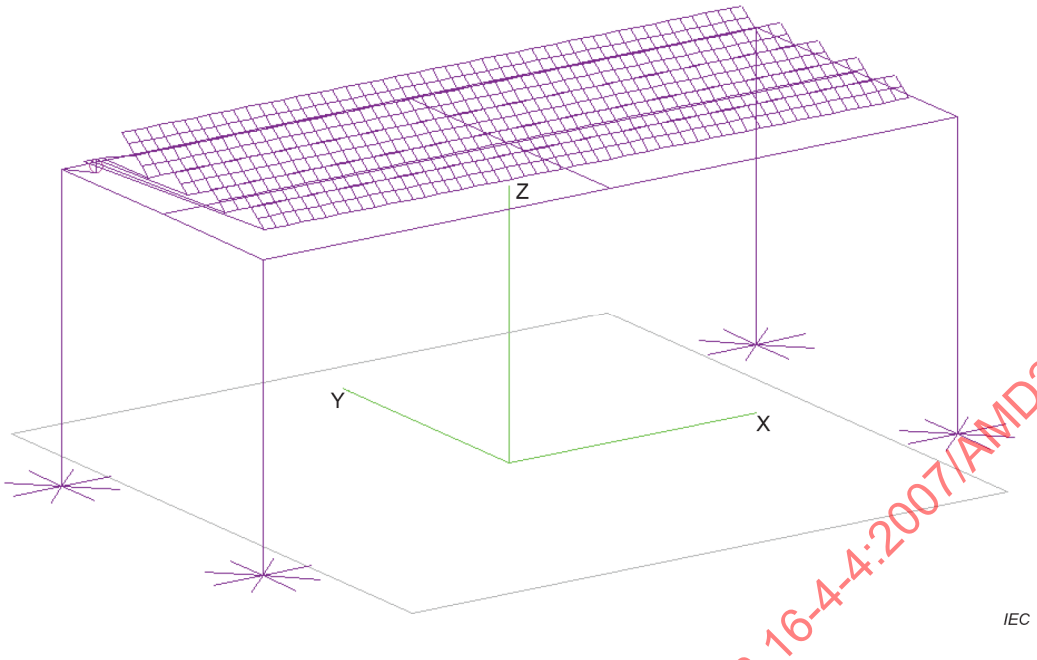

Figure C.9 – Geometrical representation of Group B PV generators

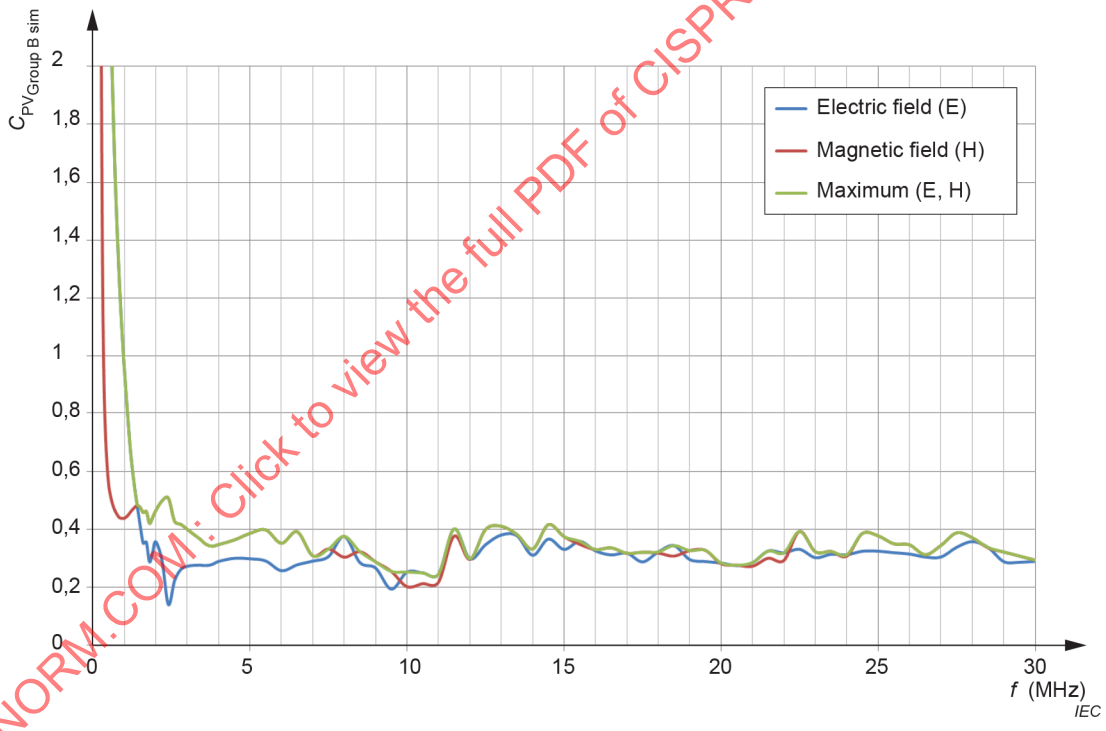

Figure C.10 – Combined coupling factor $C_{PV\,Group\,B\,sim}$ for Group B PV generators (r = 10 m)

C.3.4.1.4 Simulation results for the coupling factor $C_{PV\,Group\,C\,sim}$ – Group C (Sun tracker)

For this simulation the real installation of 7 × 4 modules and about 6 kVA was considered, while the maximum height above ground is 6,4 m and the width 7 m. The elevation angle of the PV panel plane is 30° and the centre of the plane is at a height of 5,75 m. The feed point is allocated at the bottom of the vertical DC power cable wiring. In this simulation, different Sommerfeld ground model parameters from those stated in C.3.4.1.1 were used. The values

were derived in real measurements leading to average values of conductivity σ = 20 mS/m and permittivity ε_r = 27. See Figure C.11 and Figure C.12.

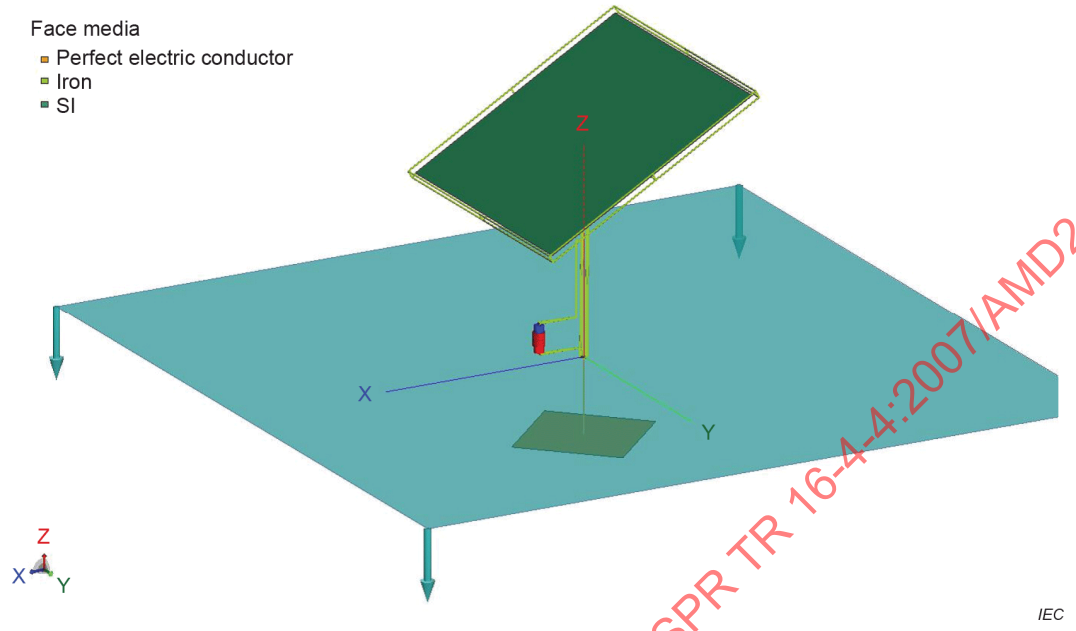

Figure C.11 – Geometrical representation of Group C PV generators

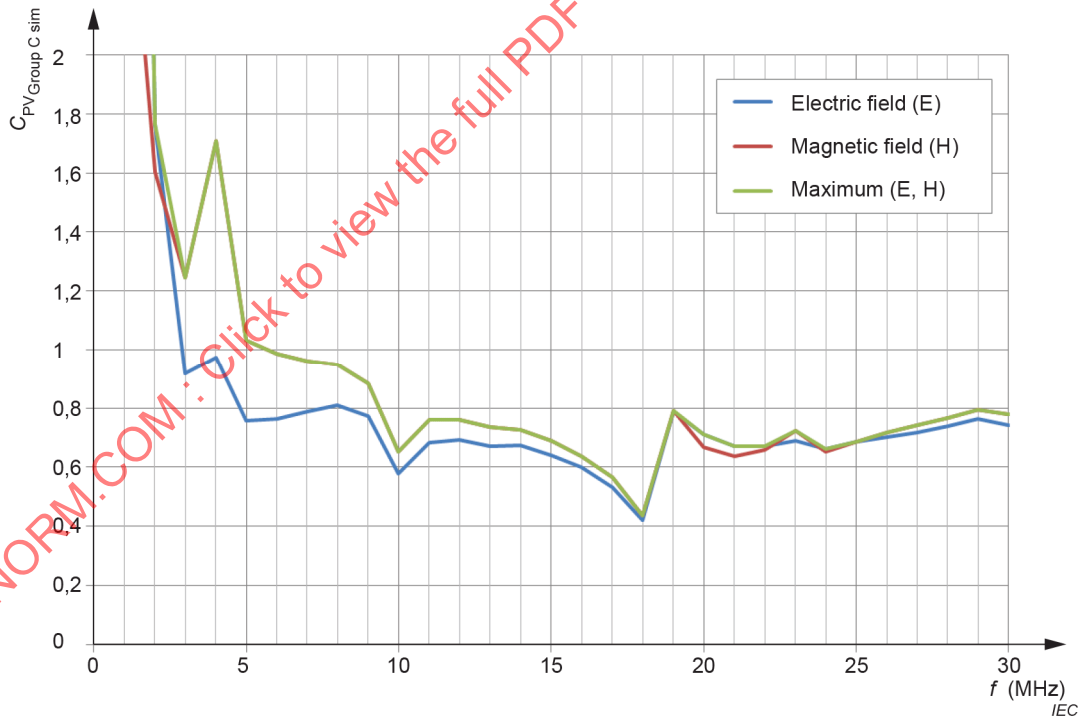

Figure C.12 – Combined coupling factor $C_{PV\,Group\,C\,sim}$ for Group C PV generators (r = 10 m)

C.3.4.1.5 Simulation results for the coupling factor $C_{\mathrm{PV\ Group\,D\,sim}}$ – Group D (Large barns)

For this simulation the total resulting power was around 12 kVA; the maximum height is not larger than 6 m. See Figure C.13 and Figure C.14.

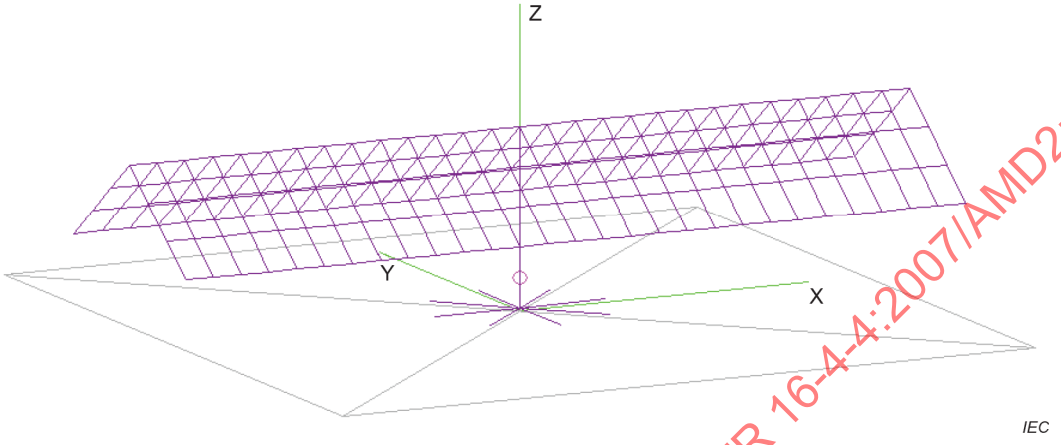

Figure C.13 – Geometrical representation of Group D PV generators

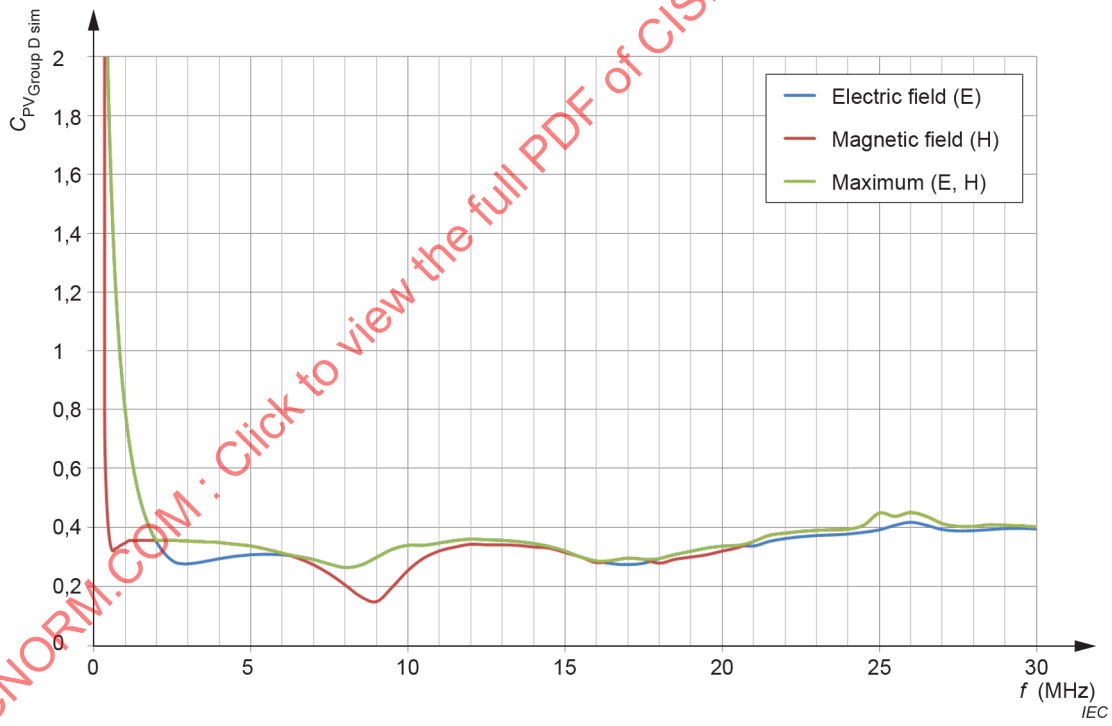

Figure C.14 – Combined coupling factor $C_{\mathrm{PV\ Group\,D\,sim}}$ for Group D PV generators (r = 10 m)

C.3.4.1.6 Coupling factor $C_{\mathrm{PV}i\,\mathrm{sim}}$ at low frequencies

For all four models (Group A to D) the simulation results for the determination of a coupling factor $C_{i\mathrm{sim}}$ between inserted power and resulting field strength at 10 m distance showed a roughly constant variation with frequency in the range from 4 MHz to 30 MHz. However, also in

all simulations a distinct increase up to very large values in the low frequency range (< 4 MHz) was observed.

Detailed investigations have shown this effect to be the result of specific software assigned feed point properties assuming ideal, non-realistic electronic components gaining increasing significance in the low frequency range for small objects compared to the wavelength when power matched. A correction routine considering losses in the power matching network assumed by the simulating engine was introduced that provides an effective solution for a refined calculation in the critical frequency range from 150 kHz to 5 MHz.

C.3.4.1.7 Overview of $C_{PV_{i\,sim}}$ for the different groups of PV generators

With the artificial effect of a high increase of the coupling factor at low frequencies being compensated by the introduced correction routine (C.3.4.1.6), the coupling factor for each group can be represented by one non-frequency dependent average value (see Table C.1).

Table C.1 – Coupling factors $C_{PV_{i\,sim}}$

PV generator group	$C_{PV_{i\,sim}}$
Group A	0,50
Group B	0,35
Group C	0,79
Group D	0,35

C.3.4.2 Determination of coupling factors $C_{PV_{i\,meas}}$ by measurement

C.3.4.2.1 General

Although for the reasons described in C.2.4.3 this task is rather complex, measurements on three real installations could be carried out. In the subsequent evaluation process the objects were assigned to each represent one of the Groups A, C and D.

C.3.4.2.2 Description of the measurement setup

Figure C.15 shows a schematic representation of the measurement setup.

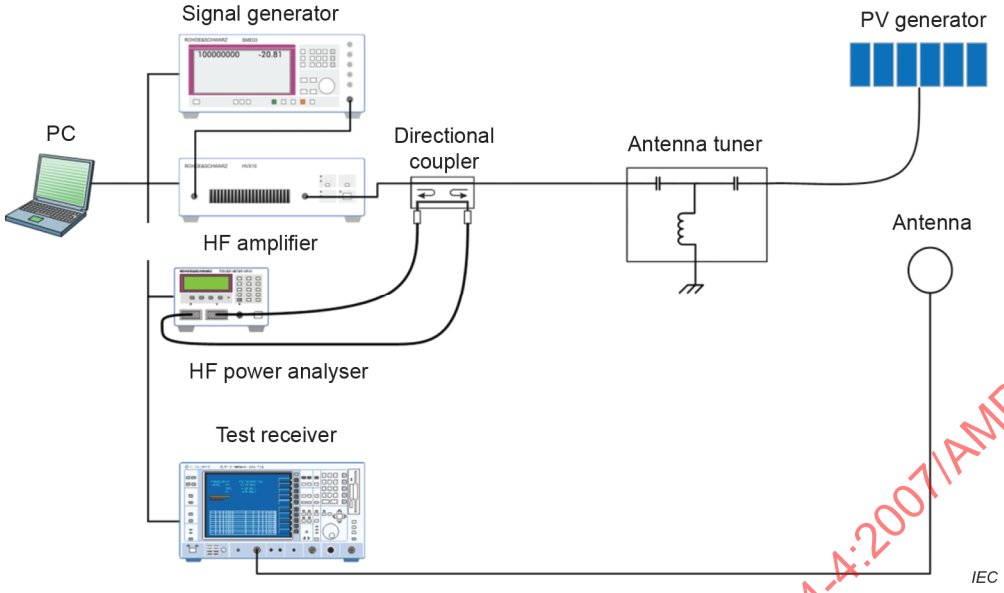

Figure C.15 – Measurement setup

A radio frequency signal was produced by a computer controlled signal generator and amplified to about 40 W. The signal then passed through a bidirectional coupler to monitor the forward and reflected power to ensure that most of the power is actually radiated. The antenna tuner helped to match the photovoltaic generator to an impedance of 50 Ω. When the antenna was properly tuned the reflected power was 20 dB less than the forward power. The fed power is the difference of the forward and reflected power. Then the electric and magnetic field strengths in 10 m distance from the photovoltaic generator were measured in three orientations (see Figure C.16).

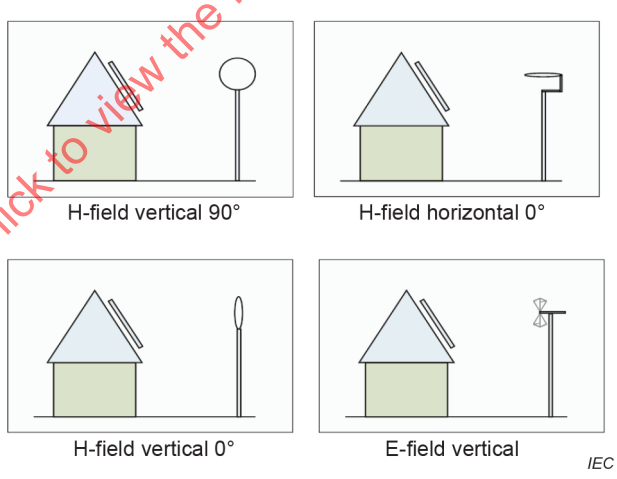

Figure C.16 – Antenna orientations

The combination of these three measurements by geometric addition delivered the final total field strength, which was then divided by the square root of the fed power. For practical reasons, data was recorded in the defined antenna positions at three different heights (h = 3,3 m, h = 5 m and h = 9,8 m).

Subclauses C.3.4.2.3 to C.3.4.2.5 give the measurement results for the three different sites including the combination procedure described in C.2.4.2. For the calculation of the final coupling factor, the data was averaged over frequency, using the data between 10 MHz and 30 MHz, where the typical non frequency dependent behaviour of the coupling factor is recognized.

C.3.4.2.3 Measurement results for the coupling factor $C_{PV\ Group\ A\ meas}$ – Group A (Single-family detached houses)

See Figure C.17.

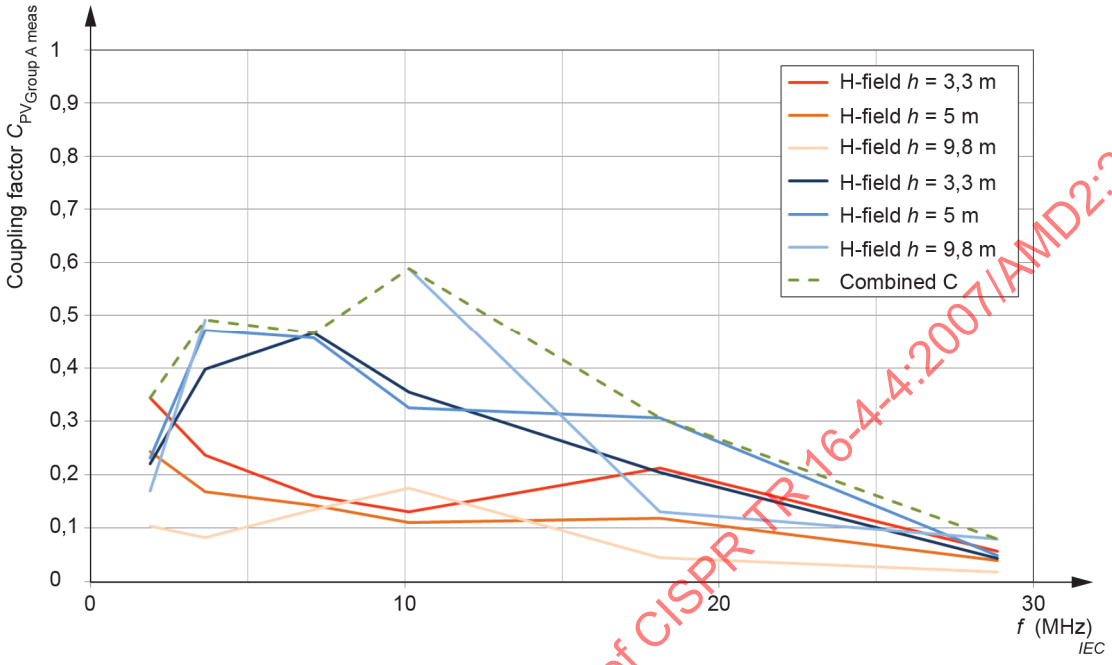

NOTE Due to a measurement error the data point E-field h = 9,8 m at 7,1 MHz is missing.

Figure C.17 – Coupling factor $C_{PV\ Group\ A\ meas}$ for Group A PV generators

C.3.4.2.4 Measurement results for the coupling factor $C_{PV\ Group\ C\ meas}$ – Group C (Sun tracker)

See Figure C.18.

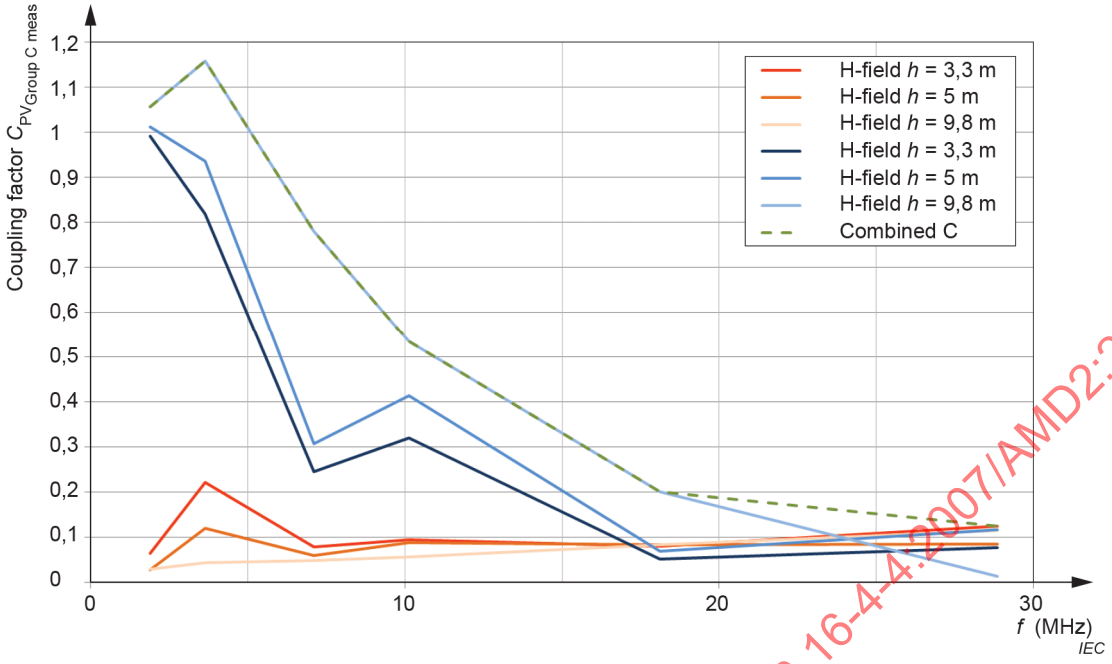

Figure C.18 – Coupling factor $C_{PV\,Group\,C\,meas}$ for Group C PV generators

C.3.4.2.5 Measurement results for the coupling factor $C_{PV\,Group\,D\,meas}$ – Group D (Large barn)

See Figure C.19.

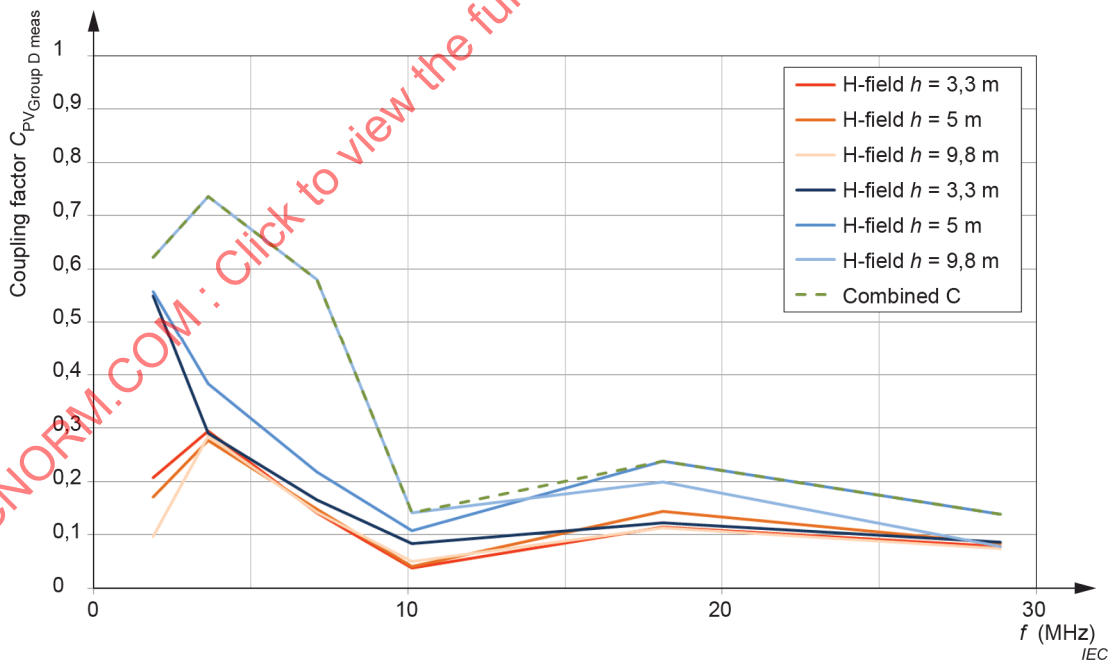

Figure C.19 – Coupling factor $C_{PV\,Group\,D\,meas}$ for Group D PV generators

C.3.4.2.6 Overview of $C_{PV_{i\,meas}}$ for the different groups of PV generators

Table C.2 – Coupling factors $C_{PV_{i\,meas}}$ and calibration factors

PV generator group	$C_{PV_{i\,meas}}$	$cal_{PV_{i\,meas}}$
Group A	0,32	0,65
Group B	-	-
Group C	0,29	0,36
Group D	0,17	0,49

The calibration factor for each individual group was calculated by division of the measured and simulated coupling factor. As overall calibration factor the average of those individual calibration factors was taken resulting in a value of 0,5. This factor was used to correct for losses of a solar generator in a real environment with respect to the simulation results. See Table C.2.

C.3.4.2.7 Consolidated coupling factors (C_{PV_i})

Coupling factors were determined by simulation ($C_{PV_{i\,sim}}$) and measurement ($C_{PV_{i\,meas}}$). Table C.3 summarizes the results.

Table C.3 – Overview coupling factors C_{PV_i}

PV generator group	$C_{PV_{i\,sim}}$	$C_{PV_{i\,meas}}$	C_{PV_i}
Group A	0,50	0,32	0,25
Group B	0,35	-	0,18
Group C	0,79	0,29	0,36
Group D	0,35	0,17	0,18

Generally it has to be stated that, in context with the rather complex basic model, measurement as well as simulation is subject to various influence factors that cannot be covered completely. However, the findings of both evaluations being in the same order of magnitude indicates good correlation of the methods in this present case. The method of averaging was chosen to represent, as near as possible, the smallest deviation between both – measurement and simulation – while keeping the worst case approach. Additionally, a calibration of the simulated figures was done by multiplying the overall calibration factor with the individual simulation results to achieve a combination of both methods.

C.3.4.3 Determination of the global coupling factor $\overline{C}_{PV}$

C.3.4.3.1 General

As the limits for the LV DC power port of power converters have not been determined taking into account different groups of PV systems, for the verification of the limits a group-independent mean value for the coupling factor and its variance is required.

In Subclause C.3.4.3, statistical data on the population density of PV generators in the field is used to draw conclusions on such a global coupling factor.

C.3.4.3.2 Determination of the distribution factors ρ_i from statistical data of PV generators in the field

In C.2.3.3 characteristic groups of PV generators were defined.

To be able to fill the model with suitable values of ρ_i, i.e. describing the probability of an individual PV generator of being in group *i*, statistical data on the distribution of PV generator types (group and ideally type of GCPC) in the field is needed.

Representative data on these parameters on a worldwide basis is difficult to obtain.

However data on the installed nominal power of PV systems in various countries is rather easy to acquire, as the operator of a PV generator site is obligated to register to be entitled to claim for remuneration for feeding into the public network.

Figure C.20 shows the ratio of registered PV power generating systems in Germany.

NOTE 1 Data from the German Federal Network Agency (2009 to February 2015 (1 038 697 entries)). The database does only include grid-connected installations. The database does not consider changes (deactivation of sites, subsequent corrections, etc.).

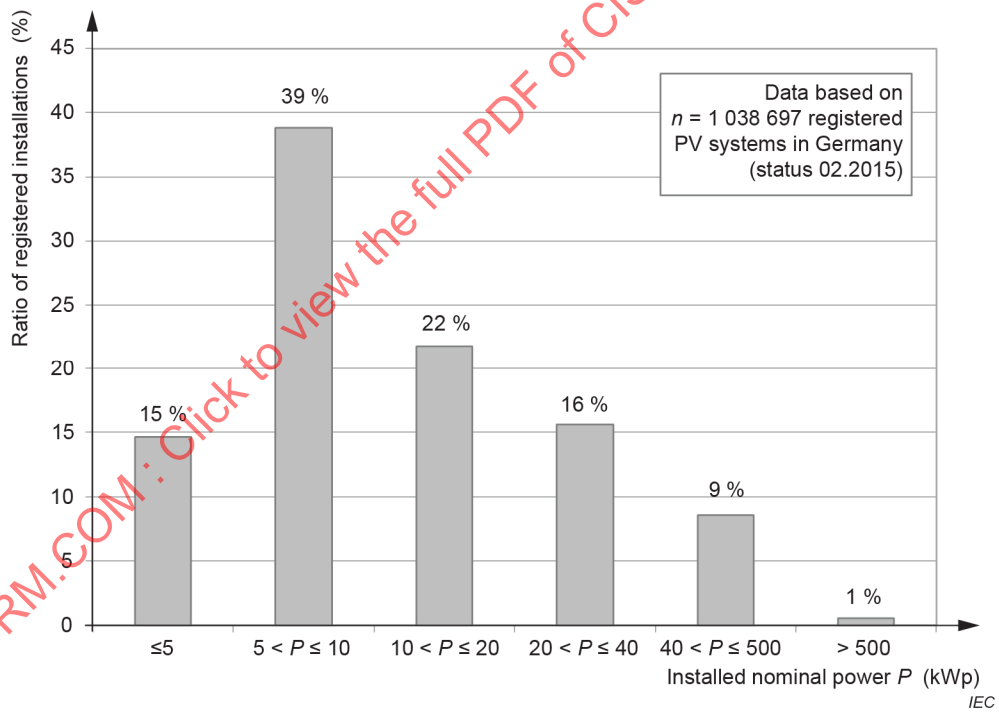

Figure C.20 – Ratio of registered PV power generating systems in Germany

Figure C.21 shows the ratio of registered PV power generating systems in Sweden.

NOTE 2 Data from the Swedish Energy Agency (2009 to 2016 (3 813 entries)). The database does only include grid-connected installations. The database does not consider changes (deactivation of sites, subsequent corrections, etc.).

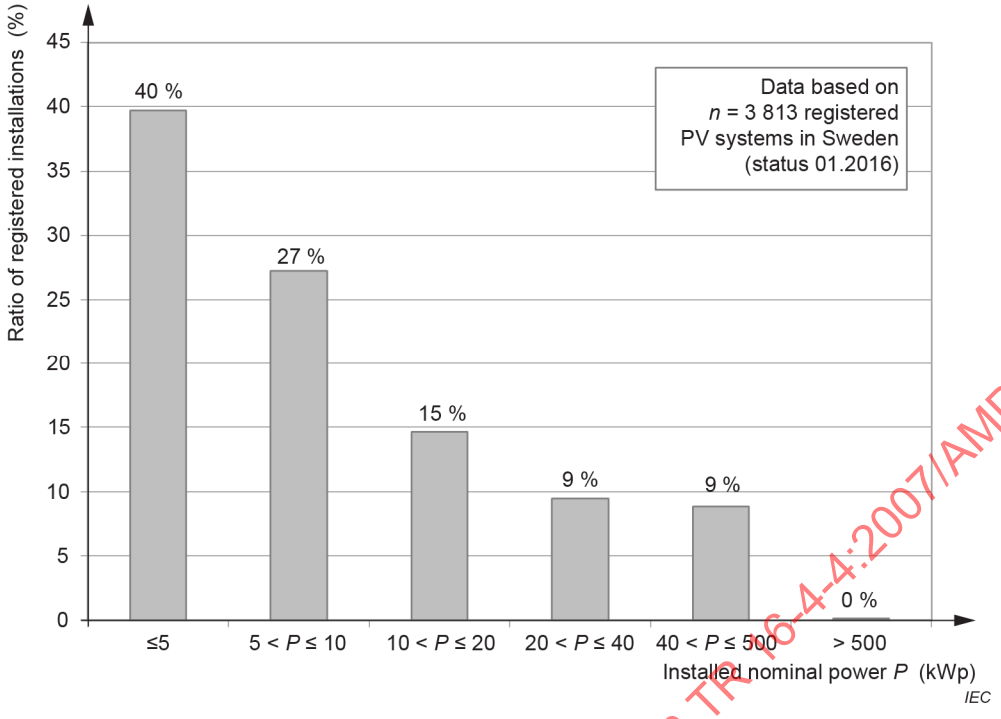

Figure C.21 – Ratio of registered PV power generating systems in Sweden

The PV systems with a nominal installed power of up to 20 kWp representing the major part of all systems with a ratio of 76 % (Germany) and 82 % (Sweden), can be supposed to be mainly applications assignable to Group A and Group B.

To obtain suitable values of ρ_i, the following estimation was performed on how the predefined groups are presumably represented in the installed nominal power ranges and subsequent weighting with respect to the particular power range (see Table C.4).

Table C.4 – Estimation of ρ_i

		Installed nominal power *P* [kWp]			
		≤ 5	5 < *P* ≤ 10	10 < *P* ≤ 20	
	Part of the entirety of PV systems with installed nominal power *P* ≤ 20 kWp ***(from statistical data)***	0,19	0,52	0,29	**Estimated ρ_i**
Estimated part of PV systems in the respective range of installed nominal power	**Group A – Single-family detached houses**	0,9	0,45	0,15	0,5
	Group B – Multi-storey buildings with flat roof tops	0	0,45	0,5	0,316 7
	Group C – Sun tracking supports (“trees”)	0,1	0,05	0	0,05
	Group D – Large barns in the countryside	0	0,05	0,35	0,133

NOTE 3 All values are given as dimensionless quantities; respective entirety of all parts is represented by value 1.

These values will be used in the following for the determination of the global coupling factor $\overline{C}_{PV}$ (see C.3.4.3.3).

C.3.4.3.3 Estimation for a global coupling factor $\overline{C}_{PV}$

Application of Equation (C.4) using the coupling factors spelled out in C.3.4.2.7 and the distribution factors ρ_i determined in C.3.4.3.2 will result in an estimation for a global coupling factor $\overline{C}_{PV}$ (Equation (C.26)).

$$\overline{C}_{PV} = \sum_{\text{all groups}} C_{PVi} \times \rho_i = 0{,}22 \frac{\sqrt{\Omega}}{\text{m}} \tag{C.26}$$

C.3.5 Determination of the maximum permissible disturbance power P_L injected into the PV generator

According to Equation (C.7) the maximum permissible disturbance power P_L can be derived by combining the function E_{Limit} with the global coupling factor $\overline{C}_{PV}$ for each frequency.

EXAMPLE For the example of the shortwave radio broadcast service in the 31 m-band introduced in C.3.2, the permissible power can be calculated. Using 33,6 dBµV/m as permissible field strength, which converts to 47,9 µV/m the following is obtained:

$$P_L = \frac{E_{Limit}^2}{\overline{C}_{PV}^2} = \frac{\left(47{,}9 \frac{\mu\text{V}}{\text{m}}\right)^2}{\left(0{,}22 \frac{\sqrt{\Omega}}{\text{m}}\right)^2} = -43{,}2\,\text{dBm} = 0{,}047\,\mu\text{W} \tag{C.27}$$

C.3.6 Consideration of mismatch conditions for the verification of the limits

The available data base for relevant factors of the mismatch conditions (m_{TC} and m_L introduced in C.2.5) being rather weak, the following options for consideration in the verification process were noted:

a) ignore assumptions for realistic mismatch conditions and calculate the worst case (i.e. maximum power matching in the test case and at the site of the installed PV generator);
b) determine typical mismatch losses by (impedance) measurements on PV generator installations and GCPCs;
c) use simulation tools such as the Monte Carlo method and operate with reasonable variation ranges for the complex load and source impedances of the PV generators and GCPCs.

During the measurements of the coupling factor $C_{PV_{i\,meas}}$ (C.3.4.2), the complex output impedance of the GCPC (Z_S) and of the PV generator (Z_L) were measured. On the three different sites (real objects) the impedance values were taken at 100 different frequency points altogether covering the interval from 150 kHz to 30 MHz. The sites represent the Groups A, C and D and were used to calculate the mismatch losses over frequency using the equations given in C.2.5.2 and C.2.5.3. As expected, the mismatch loss factors vary depending on the individual frequency. However, as this consideration is based on a statistical process, averaging of those loss factors over frequency is feasible.

For the simulation some assumptions have to be made prior to calculation. In the test case the load impedance Z_{TC} is fixed at 150 Ω, while the source impedance Z_S is unknown. Theoretically any source impedance would be possible, but realistically part of the complex plane is likely to cover typical cases. From the measurement results it can be concluded, that no source impedance has been outside the interval for the real part between 1 Ω and 1 000 Ω and for the

imaginary part −1 000 j Ω and 1 000 j Ω. Therefore this interval was chosen for the statistical determination of m_L.

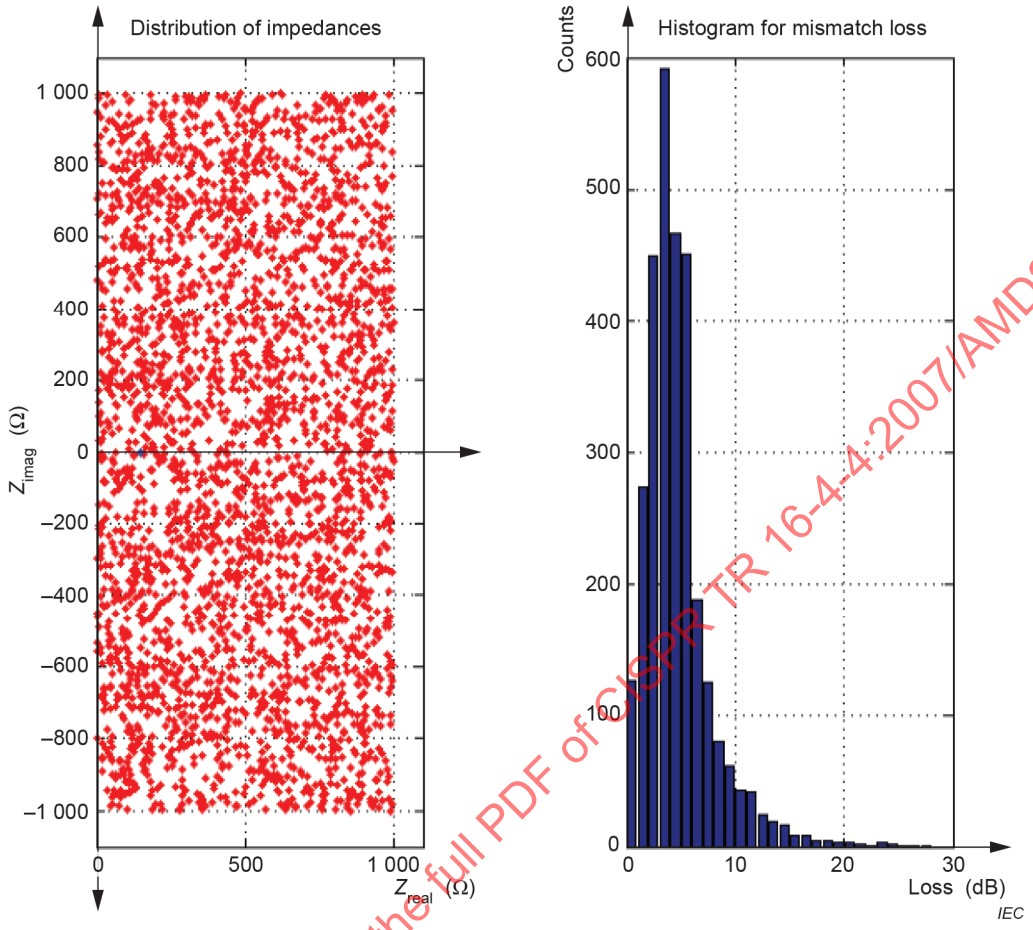

Figure C.22 – Simulation results m_{TC} (test case)

The left diagram in Figure C.22 shows the randomly distributed load impedances (red) in part of the complex plane, while the load impedance in the test case is fixed (blue dot at 150 Ω). The right diagram in Figure C.22 shows the number of impedance pairs resulting in a dB-bin.

Also for the use case an assumption is needed for the load impedance Z_L presented by the PV generator. Guidance was given by the measurement results, which exclusively show values in an interval of 5 Ω to 500 Ω for the real part and −1 000 j Ω and 1 000 j Ω for the imaginary part.

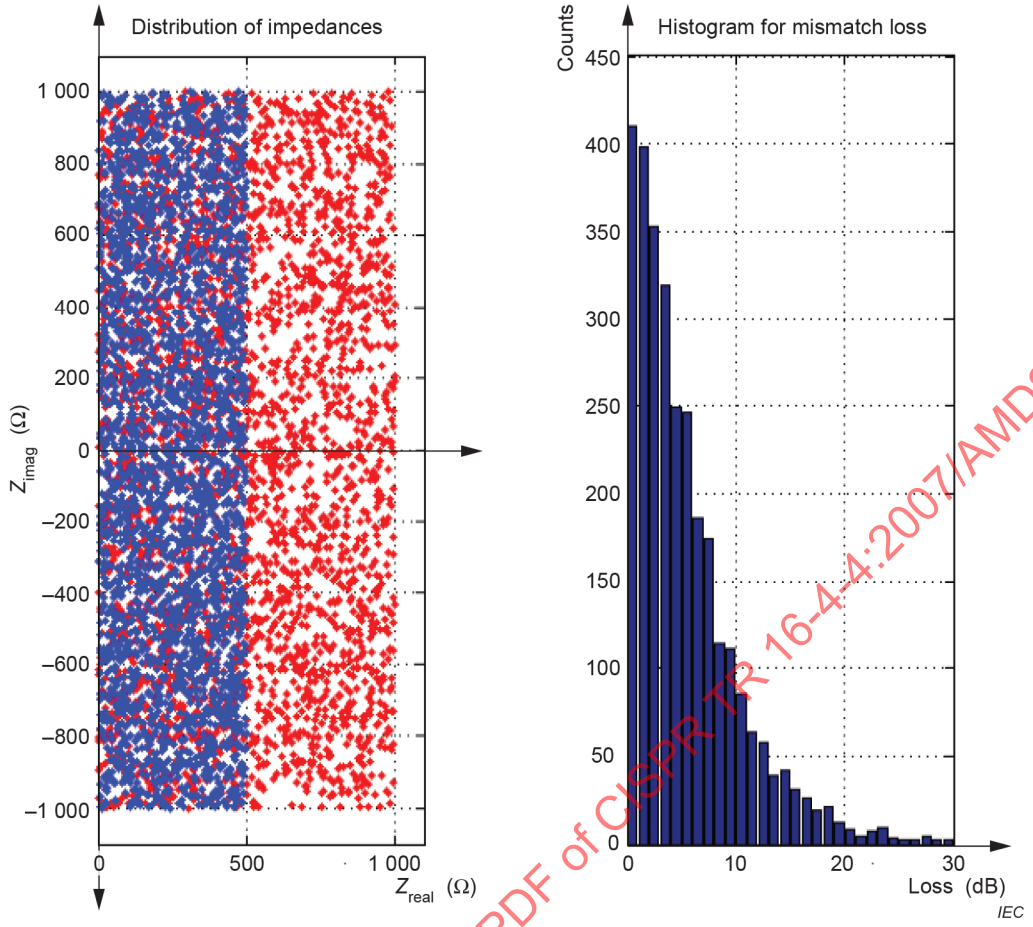

Figure C.23 – Simulation results m_L (use case)

The left diagram in Figure C.23 shows the randomly distributed source (blue) and load (red) impedances in part of the complex plane. The right diagram in Figure C.23 shows the number of impedance pairs resulting in a dB-bin. Most random pairs result in a rather low loss value.

Table C.5 gives an overview on the results determined from measurement and simulation and the combined average values of both approaches.

Table C.5 – Mismatch loss values m_L and m_{TC} determined by measurement and simulation

		m_{TC}	m_L
Measurement	Group A	0,74	0,45
	Group C	0,58	0,58
	Group D	0,20	0,06
	Average of all groups	**0,51**	**0,36**
Simulation	Monte Carlo	**0,40**	**0,43**
Combined	Average	**0,455**	**0,395**
	Average [dB]	3,42	4,03

The calculation results in the combined average mismatch factor of m_{TC} = 0,40 for the test case and of m_L = 0,43 for the use case. Both values are very close together and of the same order of magnitude as the averaged measurement result.

For the task of limit verification the combined average values of simulation and measurement are used (m_{TC} = 3,42 dB and m_L = 4,03 dB). However, it can be stated, that the approach of ignoring the mismatch situation would not be connected with great impact on the result as the determined corrections in this evaluation are rather small (below 1 dB).

C.3.7 Calculation of $U_{TC\ Limit}$ for radio services and applications in the frequency range from 150 kHz to 30 MHz

In a last step, from the calculated maximum permissible power in the test case $P_{TC\ limit}$ the disturbance voltage limit for type tests on GCPCs at test sites $U_{TC\ Limit}$ was derived using Equation (C.17).

Table C.6 gives an overview of the most important parameters (determined according to the procedure described in C.3.1 to C.3.6) for well-established radio services in the frequency range from 150 kHz to 30 MHz.

For each radio service a representative $U_{TC\ limit}$ ($f_{radio\ service}$) value was calculated based on its specific model input parameters (see Figure C.24).

Table C.6 – Calculation of $U_{TC\ Limit}$ for radio services between 150 kHz and 30 MHz at a distance of d = 10 m

Frequency [MHz]	E_w [dBµV/m]	R_P [dB]	Service	E_{ir} [dBµV/m]	μ_{P7} Time [dB]	σ_{P7} Time [dB]	μ_{P8} Location [dB]	σ_{P8} Location [dB]	μ_{P4} Frequency [dB]	σ_{P4} Frequency [dB]	E_{Limit} [dBµV/m]	$\overline{C}_{PV}$ Global coupling factor [Ω/m]	P_L [dBm]	$P_{TC\ Limit}$ [dBm]	$U_{TC\ Limit}$ [dBµV]
0,20	72	30	LF	42,0	3,8	2	8	3	10	5	58,6	0,22	-18,2	-17,6	94,1
0,28	71	30	LF	41,0	3,8	2	8	3	10	5	57,6	0,22	-19,2	-18,6	93,1
0,48	-1	10	AmaR	-5,8	3,8	2	38	6	10	5	39,4	0,22	-37,5	-36,9	74,9
1,00	60	30	MF	30,0	3,8	2	8	3	10	5	46,6	0,22	-30,2	-29,6	82,1
1,91	-3	10	AmaR	-7,8	3,8	2	38	6	10	5	37,4	0,22	-39,5	-38,9	72,9
3,75	-6	10	AmaR	-10,8	3,8	2	38	6	10	5	34,4	0,22	-42,5	-41,9	69,9
3,95	47	27	HF	20,0	3,8	2	8	3	10	5	36,6	0,22	-40,2	-39,6	72,1
5,95	45	27	HF	18,0	3,8	2	8	3	10	5	34,6	0,22	-42,2	-41,6	70,1
6,10	45	27	HF	18,0	3,8	2	8	3	10	5	34,6	0,22	-42,2	-41,6	70,1
7,15	-8	10	AmaR	-12,8	3,8	2	38	6	10	5	32,4	0,22	-44,5	-43,9	67,9
7,25	45	27	HF	18,0	3,8	2	8	3	10	5	34,6	0,22	-42,2	-41,6	70,1
7,33	45	27	HF	18,0	3,8	2	8	3	10	5	34,6	0,22	-42,2	-41,6	70,1
9,45	44	27	HF	17,0	3,8	2	8	3	10	5	33,6	0,22	-43,2	-42,6	69,1
9,70	44	27	HF	17,0	3,8	2	8	3	10	5	33,6	0,22	-43,2	-42,6	69,1
10,13	-10	10	AmaR	-14,8	3,8	2	38	6	10	5	30,4	0,22	-46,5	-45,9	65,9
11,63	43	27	HF	16,0	3,8	2	8	3	10	5	32,6	0,22	-44,2	-43,6	68,1
11,80	43	27	HF	16,0	3,8	2	8	3	10	5	32,6	0,22	-44,2	-43,6	68,1
12,05	43	27	HF	16,0	3,8	2	8	3	10	5	32,6	0,22	-44,2	-43,6	68,1
13,60	43	27	HF	16,0	3,8	2	8	3	10	5	32,6	0,22	-44,2	-43,6	68,1
13,70	43	27	HF	16,0	3,8	2	8	3	10	5	32,6	0,22	-44,2	-43,6	68,1
13,87	43	27	HF	16,0	3,8	2	8	3	10	5	32,6	0,22	-44,2	-43,6	68,1
14,18	-11	10	AmaR	-15,8	3,8	2	38	6	10	5	29,4	0,22	-47,5	-46,9	64,9
15,35	42	27	HF	15,0	3,8	2	8	3	10	5	31,6	0,22	-45,2	-44,6	67,1
15,70	42	27	HF	15,0	3,8	2	8	3	10	5	31,6	0,22	-45,2	-44,6	67,1

Frequency [MHz]	E_w [dBµV/m]	R_P [dB]	Service	E_{ir} [dBµV/m]	μ_{P7} Time [dB]	σ_{P7} Time [dB]	μ_{P8} Location [dB]	σ_{P8} Location [dB]	μ_{P4} Frequency [dB]	σ_{P4} Frequency [dB]	E_{Limit} [dBµV/m]	$\overline{C}_{PV}$ Global coupling factor [Ω/m]	P_L [dBm]	$P_{TC\ Limit}$ [dBm]	$U_{TC\ Limit}$ [dBµV]
17,50	42	27	HF	15,0	3,8	2	8	3	10	5	31,6	0,22	-45,2	-44,6	67,1
17,80	42	27	HF	15,0	3,8	2	8	3	10	5	31,6	0,22	-45,2	-44,6	67,1
18,10	-12	10	AmaR	-16,8	3,8	2	38	6	10	5	28,4	0,22	-48,5	-47,9	63,9
18,95	41	27	HF	14,0	3,8	2	8	3	10	5	30,6	0,22	-46,2	-45,6	66,1
21,23	-13	10	AmaR	-17,8	3,8	2	38	6	10	5	27,4	0,22	-49,5	-48,9	62,9
21,65	41	27	HF	14,0	3,8	2	8	3	10	5	30,6	0,22	-46,2	-45,6	66,1
24,94	-14	10	AmaR	-18,8	3,8	2	38	6	10	5	26,4	0,22	-50,5	-49,9	61,9
26,00	40	27	HF	13,0	3,8	2	8	3	10	5	29,6	0,22	-47,2	-46,6	65,1
28,80	-16	10	AmaR	-20,8	3,8	2	38	6	10	5	24,4	0,22	-52,5	-51,9	59,9

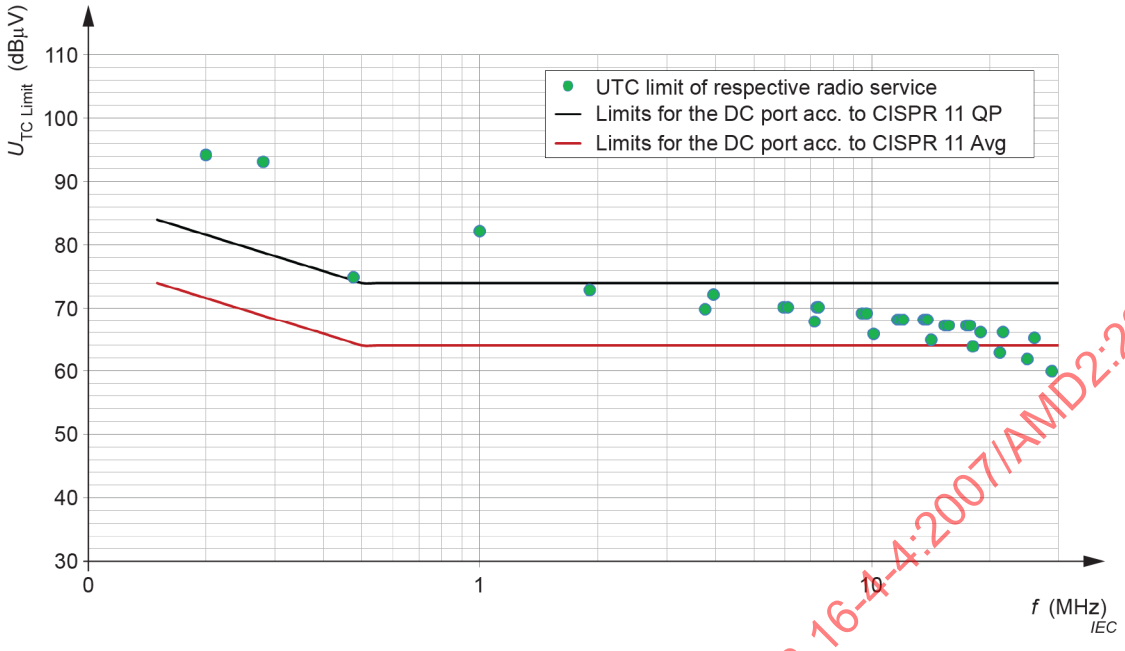

Figure C.24 – Overview of the calculated $U_{TC\ Limit}$ values for radio services between 150 kHz and 30 MHz at a distance of d = 10 m

The analysis of the green dots in Figure C.24, each representing a radio service from the radio service database, implies to average the values over frequency in order to obtain a horizontal limit line as existing in CISPR 11. Omitting the values of the first three radio services as the limit is sloping in this frequency range a value of $\overline{U}_{TC\,Limit}\left(f_{radio\ services}\right) = 67{,}9\ \text{dBµV}$ is obtained for the average detector.

Although the application of the introduced model was based on various input parameters and contains many statistical processes, it leads to a calculated limit value comparable to the established limit in CISPR 11.

Annex D
(informative)

Model for the estimation of radiation from in-house extra low voltage (ELV) lighting installations

D.1 Overview

D.1.1 Content and scope

This annex presents the method used to verify the limits set for extra-low voltage (ELV) lamps at their terminal connector which were introduced in CISPR 15:2013/AMD1:2015[1][14] and included in the subsequent edition of CISPR 15 published in 2018. This annex presents a model for estimation of the radiated disturbance from (ELV) lighting installations that are typically applied in residential environments. The modelling is limited to the radio frequency range from 9 kHz to 30 MHz.

The model is based on theoretical assumptions. Numerical simulation is used for exercizing the models.

The model is limited to disturbances arising from a single unit of an ELV lamp. Aggregation effects of multiple ELV lamps in an installation are not addressed. This annex does not consider the effects of disturbances from ELV power sources that are used to supply ELV lamps

D.1.2 Application configurations of ELV lamps

ELV lamps are usually small-sized lamps (MR 16 type) that are connected via a two-wire ELV cable to a power source. The power source is usually an electronic or magnetic transformer that is fed via the low-voltage AC mains network. Typical applications are shown in Figure D.1.

Normally, one or more of these ELV lamps are applied in a luminaire in which each lamp is connected via a two-wire cable to the power source. The two individual leads of the ELV cable run closely together inside the luminaire (Figure D.1a)). Sometimes, ELV lamps are connected in an arbitrary distributed way to a flexible rail installation below a ceiling or on a wall as shown in Figure D.1b). The two wires or metal bars of the rail system provide the ELV connection from each lamp to the power source.

1 Withdrawn.

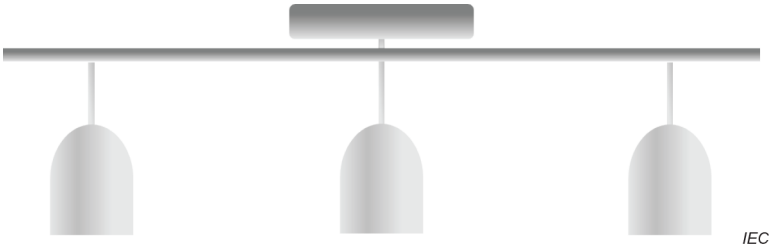

a) ELV lamps applied in a luminaire

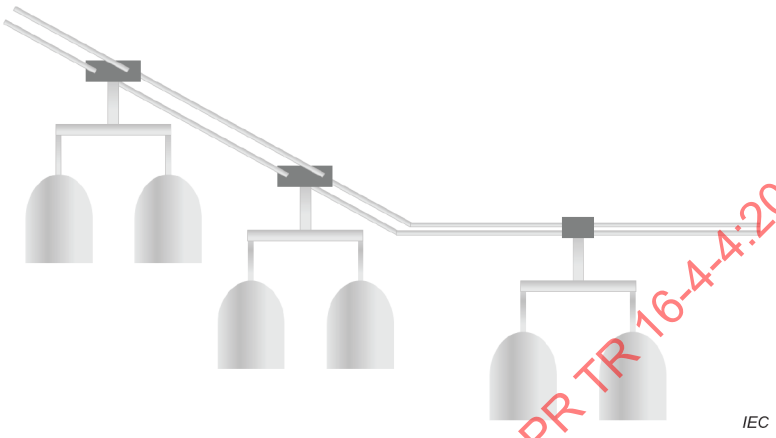

b) ELV lamps applied in a flexible rail installation

Figure D.1 – Application of ELV lamps

D.1.3 Potential interference from ELV lamps

Previous types of ELV lamps were passive tungsten halogen lamps which were fed via an AC magnetic transformer. A typical circuit is shown in Figure D.2. In the past there was no risk for radio disturbance from these passive halogen ELV lamps and the 50 Hz or 60 Hz magnetic transformers. In the past decade the magnetic transformers have been replaced by small-sized electronic transformers. Furthermore, ELV halogen lamps have been replaced by active LED-lamps. As a result, electronic (LED) ELV-lamps could potentially cause radio disturbances via the ELV wiring it is connected to. Therefore, since the publication of CISPR 15:2013/AMD1:2015 [14], specific limits have been introduced for the ELV terminals of ELV lamps.

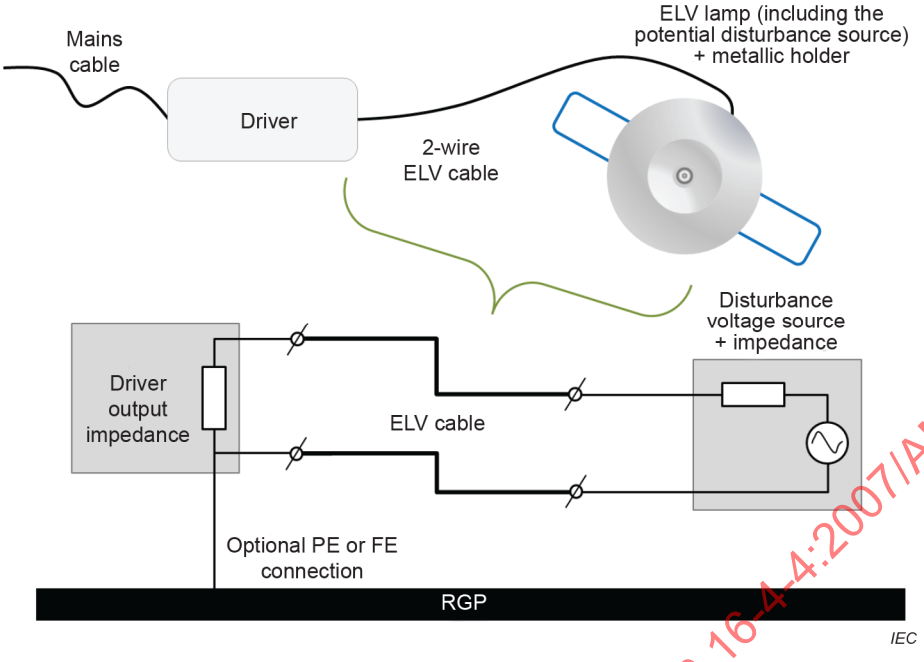

Figure D.2 – Typical components and wiring for an ELV lamp connected to a power source and the associated lumped-circuit model of the ELV part

D.1.4 Interference scenarios and associated CISPR 15 limits for ELV equipment

Figure D.3 shows the potential interference scenarios of an ELV lamp connected via an auxiliary power source to the AC mains network.

It is assumed that the lamp contains a differential-mode disturbance source with an unknown impedance.

ELV lamps are usually small and have symmetrical connections with an ELV network. It is assumed that the capacitance of the ELV lamp to the remote ground is so small, that no common mode disturbance current can be introduced via capacitive coupling of the ELV lamp.

The differential-mode disturbance current flows into a symmetric two-wire system, the two individual wires of which run parallel and have equal lengths. So, for a pure symmetrical installation, the disturbance current in each wire of the ELV cable has a phase difference of 180°. In normal luminaire applications (as depicted in Figure D.1a)) the length of the ELV wires is limited and the distance between the wires is very small.

In some more rare applications (example as depicted in Figure D.1b)), ELV lamps are connected using a flexible rail wiring system, of which the two individual wires can have a longer length, and which may be separated by a couple of centimeters. If such a rail system runs close to a conductive structure in a ceiling or wall, an unbalance may be introduced giving rise to a common-mode current.

In such practical installations, branching of the ELV wiring and application of multiple ELV lamps distributed across the wiring installation is often applied. But this will not be considered in the modelling in this annex.

Figure D.3 shows the potential interference scenarios from both the ELV part and the mains part (= low voltage – LV part) of an ELV system.

CISPR 15:2018 provides two methods for measuring disturbances from ELV lamps. Where the ELV lamps are applied with a specific power source (restricted ELV lamps), then the disturbance level of this specific combination shall be measured at the mains side of this specific power source using an artificial mains network (AMN) and the normal mains disturbance voltage limits of Table 1 of CISPR 15:2018.

If there is no restriction for the application of power sources (non-restricted ELV lamps), then the limits for conducted disturbance voltages of Table 4 of CISPR 15:2018 apply using an AMN at the ELV interface (see Table D.1). These limits are 26 dB above the Table 1 limits of CISPR 15:2018 that apply for the mains voltage (LV) disturbances. The value of 26 dB is based on the typical value of the ELV power source insertion loss of the differential mode (DM) current.

Hence, the following potential interference scenarios can be recognized from Figure D.3:

a) conducted coupling from mains disturbance currents (LV-side) to neighbouring mains connected radio receivers;

b) radiated coupling from mains disturbance currents (LV-side) to neighbouring radio receivers;

c) radiated coupling from the common mode (CM) disturbance currents in the ELV cable to neighbouring radio receivers;

d) radiated coupling from the DM disturbance currents in the ELV cable to neighbouring radio receivers;

Coupling scenarios a) and b) are covered by the normal mains disturbance voltage limits of Table 1 of CISPR 15:2018.

Coupling scenarios c) and d) are covered by the limits for conducted disturbance voltages of Table 4 of CISPR 15:2018 (using an AMN at the ELV interface). In addition, coupling scenario d) is also covered by the magnetic field limits of Table 8 or Table 9 of CISPR 15:2018, which conditionally apply (see 5.3.4.1 of CISPR 15:2018).

D.1.5 Modelling of two interference scenarios

Radiated coupling from the DM disturbance currents, i.e. scenario d) of D.1.4, in the two-wire ELV cable to the electromagnetic environment is possible, as the current is not flowing exactly at the same location, but at a separation distance *d* from the wires. The largest separation distance will also generate the highest level of the disturbance field. The model of this DM interference scenario is described in more detail in Clause D.2.

A second coupling effect can occur if the symmetry of the wire system is compromised, i.e. by a coupling to remote ground, which may be larger for one of the wires and smaller for the other wire. This would result in some conversion of DM to CM current and the ELV wiring then acts as a common mode radiator. This is coupling scenario c) of D.1.4 and is described in more detail in Clause D.3.

For modelling of the two scenarios, the separation *d* will be limited to 10 cm, as practical installations are unlikely to show larger distances (see also D.4.3).

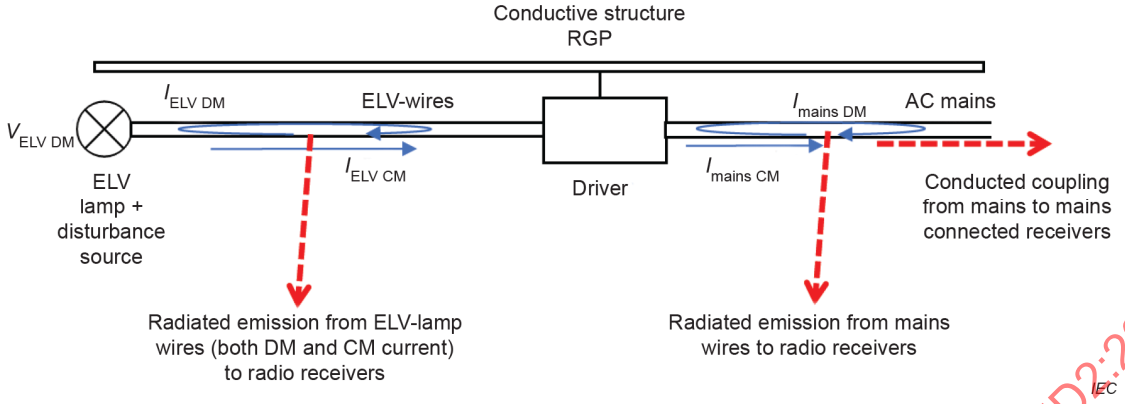

Figure D.3 – Coupling scenarios

D.2 Direct coupling of the differential mode current

Two wires with a separation distance *d* carry an equal current flowing in opposite direction as shown in Figure D.4.

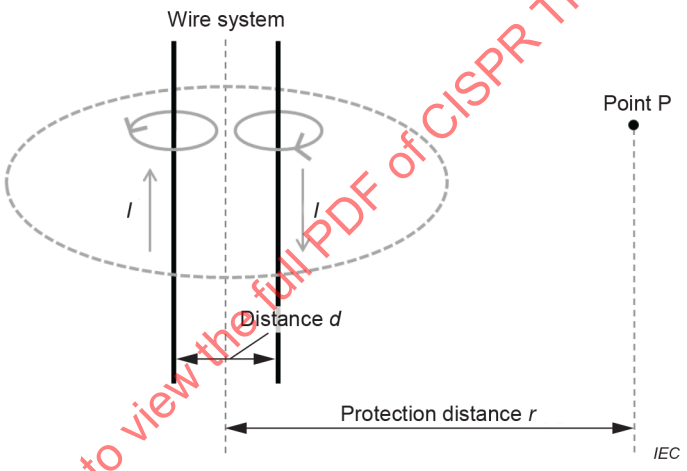

Figure D.4 – Two wire scenario

In point P, which is separated from the wire system by the protection distance *r*, both wires produce a magnetic field, which is described by the Biot-Savart-Law given in Equation (D.1).

$$H = \frac{I}{2\pi r} \tag{D.1}$$

If both wires are at the exact same distance from point P, the two magnetic field components will cancel each other out, as the current is flowing in opposite direction delivering a minus sign in the superposition of the two field components at point P. As one wire is a bit closer to point P and the other a bit further away, the cancellation is not perfect. Equation (D.2) shows the resulting field strength under the assumption that the distance between the wires is much smaller than the protection distance.

$$H = H_1 + H_2 = \frac{I}{2\pi\left(r - \frac{d}{2}\right)} + \frac{-I}{2\pi\left(r + \frac{d}{2}\right)} = \frac{I}{2\pi} \times \frac{d}{r^2 - \frac{d^2}{4}} \approx \frac{I}{\pi} \times \frac{d}{2r^2} \tag{D.2}$$